CHALMERS
UNIVERSITY OF TECHNOLOGY

Powder Flowability in Snack Food Coatings

Insights from Rheometric and Morphological Analysis

Master's thesis in Life Science

CHELSEA NYANGENA

DEPARTMENT OF FOOD AND NUTRITION SCIENCE
CHALMERS UNIVERSITY OF TECHNOLOGY

Gothenburg, Sweden 2025
www.chalmers.se

Powder Flowability in Snack Food Seasonings: Insights from Rheometric and Morphological Analysis

CHELSEA N. NYANGENA

Department of Food and Nutrition Science
Chalmers University of Technology
SE-412 96 Göteborg
Sweden
Telephone +46 (0)31-772 1000

Chalmers Reproservice
Göteborg, Sweden 2025

Powder Flowability in Snack Food Coatings:
Insights from Rheometric and Morphological Analysis

CHELSEA N. NYANGENA
Department of Food and Nutrition Science
Chalmers University of Technology

Abstract

The rheological characteristics of powders are crucial in the food industry, affecting production and product quality. This research conducted at Santa Maria AB focused on the characteristics of cheese-based snack seasoning powders' flow properties under varying formulations and environmental conditions, utilizing both rheometric and morphological assessments. It investigated silicon dioxide's impact on flowability, compared rheological traits of in-house and external suppliers' samples, assessed humidity and storage effects on flowability, and assessed morphological data of five samples. Supplementary methods such as particle sieve analysis and water activity testing were also employed for enhanced interpretation of powder behavior. Rheometric assessments utilized the FT4 powder rheometer® by Freeman Technology, while morphological evaluations were conducted by the Danish Technical Institute.

Key findings revealed that added silicon dioxide (SiO) improved flowability, agreeing with existing literature. In-house samples in the aeration test exhibited rheological similarities to external supplier samples when SiO was included.However, original in-house samples with 1.3% SiO (SM-1.3%) had lower cohesion values than external samples. This suggests that shear resistance alone does not capture the flow behavior of the seasoning but also there is a possible interplay between cohesion and adhesion. Furthermore, PCA plot of the collected data from the FT4 powder rheometer® displayed no apparent clustering among the samples but rather indicated that differences in rheological behavior could be attributed to factors that were not captured in the rheometric assessment. From the morphological assessment, findings revealed that the sample SM-1.3% was larger than SM-1.75% in terms of diameter, further strengthening the observed effect of silicon dioxide on flowability. Sample with higher silicon dioxide tended to have smaller and more spherical particles but also a narrow particle size distribution. In addition, humidity testing confirmed the impact of SiO_2 on flowability where samples subjected to higher relative humidity displayed more cohesive behavior, aligning with previous research. Lastly high shear mixers on fine powders increased cohesion and aerated energy, without improving flowability. No significant particle size distribution differences were found between low and high shear mixing, however, further replicates could provide statistical robustness.

Conclusively, results emphasized the importance of anti-caking agents such as silicon dioxide, environmental control, and the use of appropriate mixing methods for optimizing powder flow. These findings provide a framework for improving seasoning performance in industrial applications. Future research could benefit from added replicates, visual inspection such as image analysis and the influence of fat content on powder behavior to determine the influence of ingredient selection

Keywords: Powder rheology, flowability, food powder, FT4 powder rheometer®, particle morphology, mixing intensity, snack seasoning, anti-caking agents, humidity effects, adhesion

Acknowledgements

I would like to express my greatest gratitude first and foremost to my mother, Sarah for her unwavering love, support and constant encouragement. Thank you for believing in me throughout my education, your strength has always been my guiding light. I would also like to extend my gratitude to my friends and family and my supervisor Lukitawesa for his patience and thoughtful feedback.I'm grateful for your unwavering enthusiasm and insightful conversations, which have greatly aided in the success of this project. And to my managers, Martin Pollnow and Annika Ternevi, thank you for your trust, encouragement and for creating an uplifting environment. You have truly made this past 5 months very enjoyable. Lastly, I would like to express my gratitude to my examiner for providing invaluable constructive feedback and insightful evaluations. Your perspective has been helpful in enhancing and broadening the scope of this project beyond its initial scope. I deeply appreciate your role in building this project to its completion.

This achievement is a testament of the shared journey and I am incredibly thankful to each and every one of you for being a part of it.

Chelsea Nyangena, Gothenburg, June 2025

List of Acronyms

Below is the list of acronyms that have been used throughout this thesis listed in alphabetical order:

AE	Aerated Energy
AIF	Angle of Internal Friction
AIF (E)	Effective Angle of Internal Friction
AIF (SS)	Angle of Internal Friction Steady State
AOR	Angle of Repose
AR	Aeration Ratio
BFE	Basic Flow Energy
c	Cohesion
CBD	Conditioned Bulk Density
CI	Compressibility Index
CPS	Compressibility Index
ffc	Flowability
FRI	Flow Rate Index
HR	Hausner Ratio
MPS	Major Principal Stress
RH	Relative Humidity
UYS	Unconfined Yield Strength
SM	In-house sample prefix (e.g., SM-1.3%)
SP	External supplier sample prefix (e.g., SP-3)

Sammanfattning

De reologiska egenskaperna hos pulver är avgörande inom livsmedelsindustrin, då de påverkar produktion och produktkvalite. Denna studie, genomförd vid Santa Maria AB, fokuserade på flödesegenskaperna hos ostbaserade kryddpulver med varierade formuleringar och miljöförhållanden, genom användning av både reometriska och morfologiska analyser. Studien utvärderade inverkan av kiseldioxid på flödesegenskaperna, jämförde de reologiska egenskaperna hos prover tillhörande Santa Maria och prover producerade av externa leverantörer. Studien utvärderade även påverkan av luftfuktighet och lagring på flödesegenskaper samt utvärderade morfologin hos fem prover. Kompletterande metoder såsom siktanalys och vattenasktivitetstester användes för att ge en fördjupad förståelse för pulverbeteendet. De reometriska tester utfördes med hjälp av FT4 pulverreometern® från Freeman Technology medan morfologiska anlyser utfördes av den Danska Tekniksa Institutet (DTI).

De reometriska testerna utfördes med hjälp av FT4-pulverreometern® från Freeman Technology, medan morfologiska analyser utfördes av Danska Tekniska Institutet (DTI). Resultaten visade att ökad mängd kiseldioxid förbättrade flödesegenskaperna, vilket överensstämmer väl med tidigare forskning. Prover från Santa Maria (SM) med tillsats av kiseldioxid hade liknande flödesegenskaper i luftningstester som de från externa leverantörer (SP). Däremot hade SM med 1.3 % kiseldioxid (SM-1.3%) lägre värde i skjuvmotstånd jämfört med de flesta SP-prover. Detta tyder på att skjuvmotstånd ensamt inte förklarar kryddans flödesbeteende, utan att det sannolikt finns ett samspel mellan partiklar av samma slag (kohesion) och partiklar av olika komponenter i kryddpulvret (adhesion).

Sammanfattningsvis understryker resultaten vikten av anti-klumpningsmedel såsom kiseldioxid, miljökontroll, samt val av lämplig blandningsteknik för att optimera pulverflöde. Dessa resultat utgör ett ramverk för att förbättra kryddans prestanda i industriella tillämpningar. Framtida forskning skulle kunna dra nytta av fler replikat, visuell inspektion såsom bildanalys, samt studier kring fettinnehållets inverkan på pulverbeteende för att bättre förstå flödesegenskaper hos blandpulver inom livsmedelsindustrin.

Contents

List of Figures

List of Tables

1 Introduction

Powder rheology is a critical area of study within the food industry, as it directly influences the efficiency of manufacturing processes and the quality of final products[1]. However, powder as an Newtonian material, is unpredictable influenced by various parameters such as particle-level attributes (size,shape, surface roughness), interparticle forces (van der Waals, electrostatics, capillary bridges) and environmental factors such as humidity and temperature [2][3]. Several studies have been dedicated to understanding the flow behavior of powder yet little is known of the exact mechanisms behind powder flow or the interactions of the factors that influence flowability. Additionally, there is limited research on complex particle interactions and real-life applications in industrial settings based on the theoretical knowledge. This issue is particularly widespread in the food industry, where predictive knowledge about the adhesion of food powders to snack foods remains limited.

The application of different seasonings as coatings is a common practice within the snack food industry[4]. Over the past year, Santa Maria AB discovered that their cheese seasoning had poor flow properties during production, where the seasoning adhered poorly to the nacho chips. Based on the feedback from their factory, the cheese seasonings produced by their external suppliers exhibited superior performance in comparison. Non-homogeneous coating is a prevalent problem within the snack food industry as it contributes not only to decreased quality in the final product but also leads to waste production, downtime, and possible machinery maintenance problems, ultimately resulting in economic implications [5]. Therefore, increased knowledge of powder rheology is of great importance.

1.1 Aim

The aim of this study was to investigate the rheometric properties of cheese-based snack seasonings under different formulation, environmental, and processing conditions to improve powder flowability and coating efficiency. The research assessed the impact of silicon dioxide concentration on rheological properties using FT4 powder rheometer ®by Freeman Technology. Additionally, the study compared the rheological behavior of Santa Maria's in house seasoning powder to those from external suppliers to identify flow characteristics linked to improved traits associated with superior performance. Environmental influences were evaluated by simulating seasonal changes and assessing their effects on rheological properties. The study also investigated the impact of different mixing methods (low vs. high shear) on cohesion, flow behavior, and particle size distribution. Lastly, the study evaluated the difference in particle morphology of the samples, linking the findings to their flowability. The outcomes aim to establish a framework for optimizing future seasoning formulations to ensure effective powder performance.

1.2 Gaps in literature

This study adresses the lack of a multifactorial methodology for evaluating the powder behavior particularly in food applications such as cheese-based seasonings. Pre-existing literature have evaluated the influence of individual variables such as particle size, interparticle forces and environmental conditions like humidity, however these variables are often studied in isolation. This study combines rheological testing using advanced powder rheometer with morphological analysis for determining powder behavior.

1.3 Motivation for thesis work

My motivation for the thesis is based on my interest in food science, particularly in understanding how various factors may affect food quality and safety. I am eager to explore new innovative methods by combining my biotechnological principles to improve food,quality preservation but also ensure sustainability in food production. This area of study offers opportunities to also explore powder rheology in combination with food science which aligns with my academic and career goals. It also offers a crossfunctional exploration into the subject, challenging my way of thinking and other possible ways of approaching real-life problems.

1.4 Limitations

The study was limited primarily by the time frame allocated for its completion. Due to the unpredictable nature of powders, there are many potential angles from which their behavior can be analyzed. However, this research chose to focus exclusively on rheometric properties, thus only examining the physical characteristics of the powders. Additionally, most of the experiments required considerable time to complete, limiting the ability

to collect more than duplicate measurements. This influenced statistical analyses, potentially affecting the results and making definitive conclusions difficult to establish. Additional constraints included the food waste produced during testing. Because each test required a substantial amount of sample, replicates per sample were therefore limited to duplicates. In addition, investigations in the ingredients of the cheese seasonings were limited by intellectual property constraints and restricted access to confidential data. This led to limited exploration in other factors such as the effects of ingredients on powder flow.

2 Theoretical background

Powder rheology is the study of how granular bulk materials flow and deform under applied forces and stresses[6]. It examines the complex behavior of particle systems, including their flowability, cohesion, and internal friction characteristics. According to Freeman Technology, there are three phases of powders: solids in the form of particles, air that exists between the particles and liquids that are present on the surface or within the particles[7]. This three-phase composition makes powders unique materials and explains why their behavior can be challenging to predict and control in industrial settings. The subsequent sections explore the various factors that affect powder flowability and the current methodologies for determining powder flow.

2.1 Caking mechanisms and prevention

Caking represents the transformation of free-flowing particles to forms with lumps, thereby diminishing in functionality and quality[8]. It is often intensified by environmental factors such as temperature variations, relative humidity changes, storage time and mechanical pressure[9]. The underlying mechanisms differ between two material types of powders, crystalline and amorphous [10]. In 1995, Aguilera et. al defined caking of crystalline powders as a process that occurs in different stages, including bridging, agglomeration, compaction, liquefaction, and solidification [8]. A recent study by Chen et al. groups the mechanism into three distinct stages: moisture sorption, liquid bridge formation and crystal bridge development. Both articles describe caking as a progressive phenomenon moving from bridging to final solidification and recognize moisture as a primary initiator of caking.

In the initial stage, moisture absorption leads to surface deformation and sticking at contact points between particles. Moisture absorption can occur through direct absorption from the atmosphere, condensation on particles surfaces due to temperature drops or accidental wetting during processing [9]. The particles absorb moisture slowly below a specific relative humidity (RH0), but soon after progress rapidly once they surpass the RH0[10]. Thereafter, humidity can progress to two main processes: capillary condensation and deliquescence. Capillary condensation occurs when the specific relative humidity (RH0) surpasses RHcc, also known as the critical threshold. While deliquescence occurs as a result of the relative humidity surpassing the specific relative humidity (RH0). Capillary condensation forms discrete liquid bridges at particle contact points, maintaining the original particle structure while liquid formation due to deliquescence covers the entire particle surface. This can lead to particle dissolution as the liquid film grows i.e. particle dissolves into a solution[11].In the agglomeration stage, particles cluster together more tightly, changing in particle shape and size. The process is irreversible unlike the bridging stage where connections could break under mild disturbance[9]. During compaction, a significant transformation in the powder structures takes place due to increasing pressure and moisture content [8]. Particle clumps deform, resulting in a loss of the powder's original characteristics leading to either wet sticky masses or hard agglomerates in the solidification stage[9]. This results in a hard powder with poor flowability, an undesirable trait not only within the food industry but also prevalent in other industries that use powder, such as additive manufacturing and pharmaceuticals.

While caking of crystalline powders involves moisture-related mechanisms, caking of amorphous powders involves the glass transition temperature (Tg) in conjunction with moisture content. Tg is the temperature range at which amorphous materials transition from a glassy brittle state to a more "rubbery state [12]. Increased moisture content lowers the glass transition temperature and water can act as a plasticizer between particles. When the temperature exceeds the glass transition temperature, the powder decreases in viscosity[9]. Above Tg, powders rapidly develop inter-particle bridges, leading to the formation of clusters and a loss in the powder structure.

Caking in all applications is undesirable but unavoidable. Strategies to mitigate caking include environmental control and the use of anti-caking agents[10]. Moisture-induced caking can be controlled by maintaining conditions below critical relative humidity threshold (RHcc) and the specific relative humidity (RH0). Conversely, control of the temperature can also prevent the powder from caking. In the food industry, it is common to add anti-caking agents to food powders to prevent caking, lumping, and aggregation while enhancing flowability of cohesive or poorly flowing powders[13]. Anti-caking agents act as physical barriers between host particles and prevent them from coming into contact with one another. They also compete for moisture and inhibit crystal growth. Common examples include calcium silicate (E552),magnesium silicate(E553a(i)), magnesium trisilicate (E553a(ii)), talc (E553b) and silicon dioxide (E551)[13][14].In 2018, the first four food additives were re-evaluated by the European Food Safety Authority (EFSA) on their toxicity and the acceptable daily intake (ADI). Based on the evidence , none of the food additives received full safety approval for use due to insufficient data but were still approved as

food additives. Silicon dioxide as well was approved for use in the re-evaluation 2018 and remains widely used in the food industry, especially in seasonings [15]. Anti-caking agents are also known as flow aids or glidants and may be used interchangebly in this study.

2.2 Interparticle forces and mechanisms of particle interaction

Interparticle forces are the various forces acting between particles in powders [6]. They include contact forces (normal and tangential) and long-range non-contact forces such as van der Waals, capillary, and electrostatic forces. For macroscopic particles (>100 µm), contact forces dominate, while in fine particles (<100 µm), long-range forces become more significant. Contact forces as the name suggests are forces that arise from particle collision, or frictional forces. Non-contact forces, on the other hand, impose a force without direct contact with the particle. Both of these forces fundamentally determine particle behavior in processes like packing, flow, mixing, and fracture, making them crucial for understanding powder flowability.

Non-contact forces, electrostatic- and capillary charges, are dominant for small fine particles due to their higher surface-to-volume ratio, overcoming the gravity force [16][6]. This leads to stronger electrostatic interactions between particles which can significantly impact their flow behavior. Electrostatic charges also contribute to particle cohesion when the interparticle distance is reduced leading to stronger particle-particle interactions. These forces cause particles to aggregate and cake together, which significantly impacts their flow characteristics. Additionally, charged particles tend to form bridges between each other and are more likely to adhere to walls of tubes. In the end, this can cause clogging in machines and disrupt efficient performance. On the other hand, frictional forces and mechanical interlocking prevail when powder is consolidated in devices like hoppers or feeders, as a result of increased contact point density, pressure, and area[7]. Friction as a key mechanism in particle interaction is strongest for rougher particle surfaces which create more resistance to flow compared to smoother ones. In conjunction with friction, mechanical interlocking can also restrict particle movement. Particles with irregular shapes lock together and resist movement,thereby increasing in cohesion.

2.3 Powder morphology

Powder morphology refers to physical characteristics of powders such as size, shape and surface texture which all play a role in influencing powder behavior. Large particles(>100 µm) have better flowability due to a smaller surface area compared to small particles[6][17]. A larger surface area promotes interaction between particles with more contact points during moisture-induced caking and interparticle adhesion as above-mentioned. Additionally, larger particles have lower interparticle forces and cohesiveness, which reduces their stickiness to one another.Typically, powders exhibit varying particle sizes, which is characterized as particle size distribution (PSD)[18]. PSD represents the range of particle sizes in a powder and their relative proportions. The mean particle diameter, often used as a size estimator, provides a central measure of the particle dimensions within a sample [19]. Granulometric parameters such as d_{10}, d_{50}, and d_{90} are commonly calculated to describe the distribution of particle sizes. These values represent the diameters at which 10% , 50%, and 90% of the particles are smaller, respectively. In a study by Brika et al.it is noted that wider PSDs enable better particle packing as smaller particles can fill the gaps between larger particles, thereby increasing in packing density[18]. Conversely, a wide distribution leads to more contact points between particles due to the presence of smaller particles. In terms of flow performance, some studies found wider PSDs decrease flowability while others reported improved flow with broader distributions due to smaller particles acting as lubricants between larger particles[20] [21]. However, this difference in the observed flow performance can be attributed to the choice of methodology as well as the material investigated.

Besides particle size, particle shape also plays a significant role in flow performance. A study found that powders with spherical particles had better flowability due to reduced surface friction and mechanical interlocking [18]. Furthermore, smooth particles exhibit better flowability due to lower frictional interaction and mechanical interlocking[7]. Surface roughness also affects moisture sensitivity and inter-particle interactions which ultimately affect bulk powder behavior [22].

There are different methods to determine the physical characteristics of powders which include laser diffraction, particle sieve analysis, image analysis and particle morphology analysis[23] [24] [19]. Laser diffraction and particle sieve analysis determine the granulometric parameters as previously mentioned while image- and morphology analysis derive three distinct parameters: circularity, convexity and elongation. Circularity refers to how spherical

a particle is and is evaluated based on a scale from 0 to 1, where particles with a value of 1 are considered to be a perfect circle. Both particle shape and irregularities on the particle surface influence circularity. Convexity refers to how smooth a particle is and is also based on a scale from 0 to 1. The closer to 1 a particle shape is, the smoother the surface, and is determined by calculating the particle's perimeter and comparing it with the perimeter of a perfect circle of the same size. Unlike circularity, convexity is independent of the particle shape but dependent on the irregularities of the particle surface. Lastly, elongation describes how long and wide a particle is. The closer to zero a particle is, the more likeliness the particle has to a perfect circle. The elongation is independent of a particle's roughness. The figures below illustrate how to interpret results based on the various scoring.

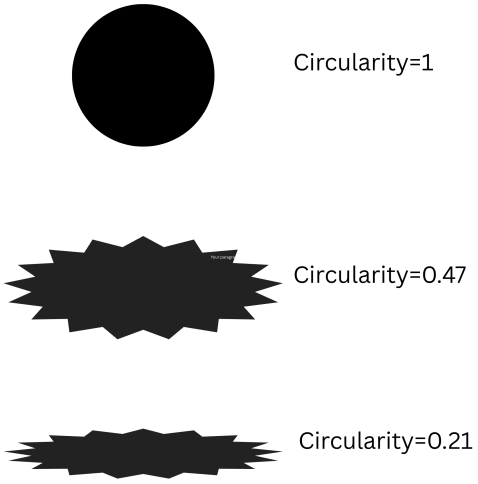

Figure 1: Illustration of different particle shapes and their interpretation in terms of circularity.Illustration is self-produced.

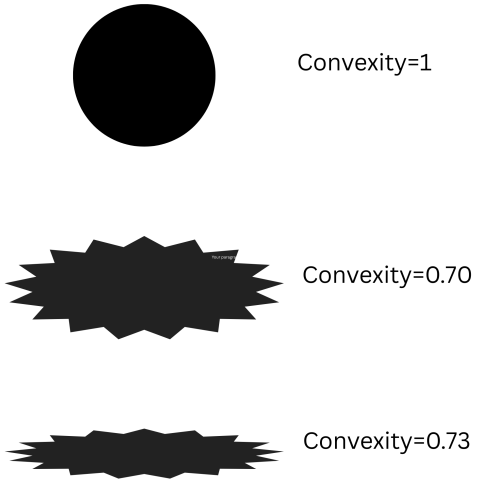

Figure 2: Illustration of different particle shapes and their interpretation in terms of convexity.Illustration is self-produced.

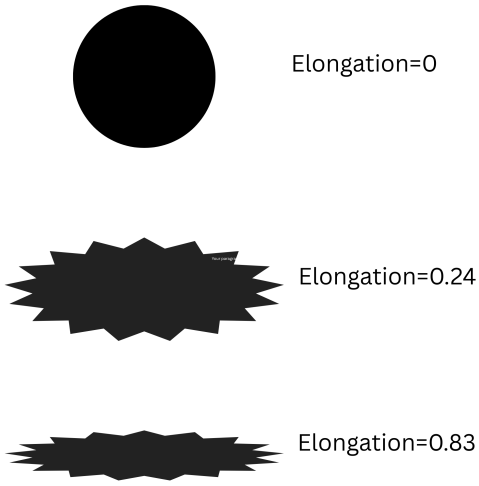

Figure 3: Illustration of different particle shapes and their interpretation in terms of elongation.Illustration is self-produced.

2.4 Methods for measuring flowability

Due to powder's unpredictable and complex behavior, no singular method exists to quantify powder flow. Angle of repose, Hausner ratio, compressibility index (CI), shear cell tests, and bulk and tapped density are some of the traditional methods that have been previously used and continue to be used to evaluate powder flowability in many industries [17]. Angle of repose is a method that measures the angle formed when a powder flows out of a funnel or is poured onto a surface[25]. The angle of repose is the steepest angle measured from the bottom of the stand against the horizontal plane of the powder from 0 to 90 °. The greater the angle, the poorer the flowability is for a certain powder. This method provides qualitative insights into the powder's cohesiveness and flow behavior. Hausner ratio (HR) is a straightforward method that assesses powder flow by measuring the tapped density and aerated density of powder [5]. It is calculated as the ratio of the tapped density to the aerated density and involves pouring the powder into a graduated vessel and tapping it a specific number of times to achieve maximum compaction. The Hausner Ratio is categorized into three different flow behavior regimes where an HR below 1.25 indicates good flowability, between 1.25 and 1.4 indicates acceptable/poor flowability, and an HR value above 1.4 indicates poor flowability. This method is used for qualitative evaluation of powder cohesiveness and flowability. The third method, compressibility index measures the volume reduction of a powder under tapping which provides insights into its flow properties[5]. CI is calculated as ratio of the difference between initial volume and volume over taps over the initial volume. Conversely, CI can also be categorised to define flowability according to Carr's classification. A good flow has a C value between 0.05 and 0.015 while a very poor flow has a value betweeen 0.35 and 0.40. Like Hausner ratio, this method is also used for evaluating cohesive materials. Lastly the shear cell test is a widely used method for evaluating the flow properties of powders. It involves applying a combination of normal and shear stresses to a powder sample to assess its flowability[17]. It is more complex and time-consuming as opposed to the other methods. In the shear cell test, measurements are done on the pre-consolidated- and consolidated stress. The results give the yield locus, which helps define the flow function (FF), angle of internal friction, and cohesion (c). The flow function describes how readily a powder flows from a consolidated stage and cohesion details the adhesive nature between different powder material layers. The Jenike classification that was proposed in 1964 and based on shear cell tests determines whether a material has good flowability based on the values:

Flow function (ff_c)	**Classification**
$1 < ff_c$	non-flowing
$1 < ff_c < 2$	Very cohesive
$ff_c < 2$	very cohesive and non-flowing
$2 < ff_c < 4$	cohesive
$4 < ff_c < 10$	easy flowing
$10 < ff_c$	free flowing

Table 1: Jenike flowability classification[26]

Advancements in technology have significantly improved the study and application of powder rheology with the invention of powder rheometers. Powder rheometers are reliable and are good for characterizing powders and predicting their performance during handling and scale-up operations. While traditional methods can indicate flowability with a single value, results are often unreliable and the methodology is heavily operator-dependent. The main advantage of powder rheometers involves their ability to test powder in moving conditions, providing realistic insights. Powder rheometers, such as the FT4 powder rheometer by Freeman Technology, provide a deeper understanding of powder behavior.

The study employs the FT4 Powder Rheometer® and data analysis software from Freeman Technology to assess the rheological characteristics of various cheese chip seasonings.Equipped with four categories of methodologies, dynamic flow, processing, bulk, and shear properties, the tests can help simulate how the powder behaves under different conditions: consolidated, loosely packed,fluidized, or aerated [27].This study explored only three out of four methodologies: dynamic flow, bulk- and shear properties. Aeration is a dynamic flow measurement that assesses how easily air can be introduced to a powder by measuring the reduction of flow energy when air is supplied into the vessel [2]. The reduction in aeration energy depends primarily on cohesion, with particle shape, texture, size and density also influencing the extent of energy reduction. Cohesive powders are generally less arable as they require more air to break apart the cohesive forces between the particles. The aeration test data

generates various parameters, with particular focus on aerated energy (AE_{xx}), where 'xx' denotes the specific air velocity which is synonymous with the total energy at a particular air velocity. The second parameter of interest is the aerated ratio (AR), a ratio of the basic flow energy (BFE) and the aerated energy at the final air velocity, where BFE is the total energy at an air velocity of zero mm/s. AR explains how sensitive the powder is to air flow. An AR value of about 1, defines the powder as insensitive to aeration. AR values ranging from 2 and 20 indicate the powder has medium sensitivity to aeration, common to most powders. Lastly, an AR value of above 20 indicates the powder is highly sensitive to aeration and will probably become fluidized, i.e the powder has low cohesive forces. Table 2 summarizes what different values of AR indicate. This study employed this method to quantify the cohesive forces between the particles.

AR value	Definition
$AR \approx 1$	Not sensitive to aeration
$2 < AR < 20$	Average sensitivity to aeration
$AR >> 20$	Highly sensitive to aeration

Table 2: Aeration ratio values with corresponding definitions.

The shear cell assesses the flowability of a powder that has previously been stored at rest and measures its flow resistance [28]. Over time, stored powders may cake due to pressure caused by the weight of the bulk material. The shear test imposes normal stress to replicate various load conditions and test at what point, denoted yield point, does the powder begin to flow [29]. The FT4 utilizes a rotational shear applying a low, gradually increasing horizontal force to a powder layer while the adjacent layer stays stationary [28]. Upon reaching a specific shear force, the upper layer slides over the lower layer. From the test data, the following parameters of interest are produced: cohesion (c), unconfined yield strength (UYS, σ_c), major principal stress (MPS,σ_1), flow function (FF), the angle of internal friction (AIF), effective angle of internal friction and angle of internal friction at steady state. Cohesion (c) defines how cohesive the powder is, with high values of c denoting a highly cohesive powder. Unconfined yield strength (UYS, σ_c), major principal stress (MPS,σ_1) are variables produced by fitting the Mohr stress circle which is a graphical representation of the internal stresses a material undergoes as a result of applied normal- and shear stresses[30]. The ratio of MPS and UYS results in the flow function (FF), which ranks the flowability of a powder according to Jenike's classification [28]. FF values below represent poor flow and above 10, the powder is easy flowing 1. Figure 4 presents the graphical representation of the Mohrs circle including the flow function as a ratio of MPS and UYS.

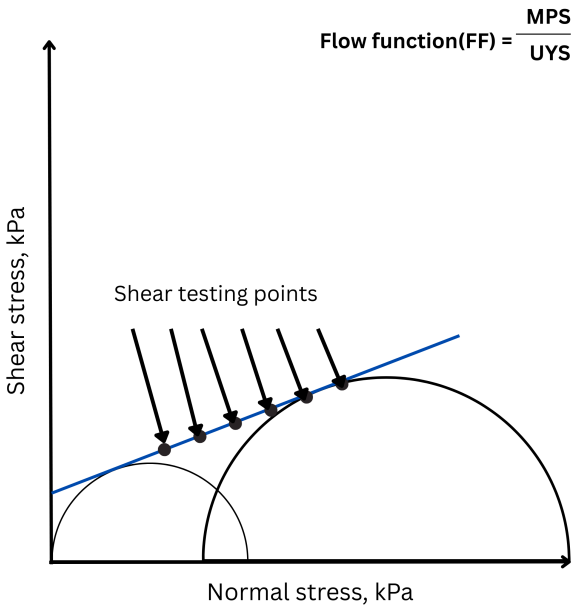

Figure 4: Illustration of the Mohrs circle. Self-produced illustration

The samples were measured at a preconsolidated stress of 6 kPa because this was the predicted pressure the samples may experience during storage. This test was conducted to determine whether storage might play a factor in the powder's decreased flowability during storage and to quantify the cohesive forces between the particles.

Compressibility measures the bulk properties of the powder by determining how density changes as a function of applied normal stress [31]. Compressibility is influenced by particle size distribution, cohesivity, particle stiffness, particle shape and particle surface texture. Essentially smaller particles are more compressible in comparison to large granular particles. Conversely, irregularly shaped particles will also be more compressible due to mechanical locking. This test helps to create a correlation between the interaction of cohesive powders and their effect in packing efficiency. Packing efficiency refers to how well the particles will occupy the spaces in the void. The test data produces a compressibility index (CPS), a function of the density over the conditioned bulk density (CBD)[31]. CBD is a ratio of the split mass after conditioning and sample volume. A high compressibility index signifies a cohesive powder with a small particle size that readily compacts upon pressure, i.e, filling up the air pockets in the powder. On the other hand, a reduced compressibility percentage demonstrates resistance to compaction, as particles are less prone to rearrange under pressure, or lacks excess air. Granular powder, i.e, powders with large particles, usually have low compressibility.

Lastly, the basic flowability energy (BFE) quantifies the energy needed to move a powder in its consolidated, non-aerated state as the blade moves downward the powder[32]. This test is suitable for understanding the powder performance when in motion. However, test data from BFE tests must be correlated with results from other tests to make accurate interpretations. According to the manual, a high BFE may indicate a powder that is highly resistant to flow, thus it is more cohesive and denser. Conversely, a low BFE may indicate a free-flowing powder with small cohesive force. However, this might also be true for a powder that may flow freely under gravity but may have a high BFE value. Therefore, BFE measurements vary across different materials, and interpretation is achieved when combined with another testing method.

In all the tests above-mentioned, a pre-conditioning step is performed to eliminate operator variability and previous consolidation effects by gently displacing the whole sample and slightly aerating the powder. The aim is to construct a homogeneously packed powder bed which results in reproducibility. In downward motion, the blade moves into the powder and upward. The conditioning cycle is also done before any test cycle as well. The only exception is when the sample is being evaluated in its consolidated state.

2.5 Humidity and moisture content

Moisture content is a critical factor influencing powder flowability during transport and storage. Powders exposed to humidity absorb water, which leads to increased cohesive forces between particles through liquid bridge formation and electrostatic effects [33] [34]. This phenomenon is particularly more apparent in hygroscopic powders such as cheese-based seasoning powders. Hygroscopic powders are granular materials that readily absorb moisture from air, resulting in stickiness and caking phenomena within the powder, significantly impairing flow behavior[8]. Hygroscopic materials have large surface areas allowing them to interact with more water vapor in the air[35]. Hausmann et al. sought to study the effect of humidity on powder flowability of sodium chloride, particularly focusing on agglomeration/caking behavior in humidity-sensitive powders[34]. They analyzed the powder flow energy under varying conditions, and findings revealed that accelerated moisture sorption was achieved by introducing humidity through the powder bed. At 80%, sodium chloride underwent deliquescence, where a crystalline solid transitions into saturated solution. Thus, resulting in significant caking and agglomeration. Therefore, relative humidity plays a key role in powder flowability.

In addition to moisture content, water activity (a_w) and temperature jointly influence caking properties of powders through their effect on glass temperature [36]. Higher water activity reduces Tg through plastization, making powders more susceptible to caking even at constant temperature.(A_w) is a crucial parameter in food science that measures the available water for biological and chemical reactions. It is defined as the ratio of water partial vapor pressure and the vapor pressure of pure water at the same temperature. The difference therefore between water content and water activity is that water content represents the total amount of moisture in a food product [37].While two foods can have the same amount of water content, the available water for reactions could differ. Thus, water activity is a better parameter for determining product stability and shelf life by controlling microbial growth and chemical reactions.

2.6 Mixer intensity

Mixing operations are factors that affect flowability and ingredient homogeneity. The use of mixers in industrial settings is important for obtaining and maintaining a quality blend [38]. Granular materials composed of different particle size need to have a uniform distribution otherwise this can lead to significant production delays and problems in downstream processes. Therefore, the understanding of mixing operations is of high importance. The intensity of the mixing operation can be categorized as low- and high-shear mixing [39]. High shear mixers are used for materials of varying densities, particle sizes or viscosities, potentially breaking larger agglomerates and coating particles more evenly. It has a high rotational speed, a sharp blade and high torque and has a high power consumption. Low shear mixers have gentler blends with lower rotational speed but the inability to break large agglomerates. Low shear mixer impellers are often larger, dull and thicker. Freeman Technology emphasizes that the use of a low shear mixer can minimize the risk of the particles breaking apart and the prevalence of eletrostatic charges[2]. On the other hand, powders with higher flow rate index, i.e. powders with poor flowability are more cohesive could benefit from a high shear mixer. Depending on the application and desired outcome, both mixing intensities offer benefits and disadvantages. High shear mixers are more suitable for emulsification, while low shear mixers are more appropriate for powder blends such as spices [38].

3 Experimental setup and methodology

This study investigated the rheological behavior of the different cheese-based seasoning powders employing various analytical techniques. Central to this study was the FT4 powder rheometer ® from Freeman Technology, supplemented by water activity measurements and particle morphology analysis. All experiments were conducted at Santa Maria AB Mölndal office except the morphology analysis that was conducted at the Danish Technical Institute. The following subsections detail the preparation and methodology used throughout the study.

3.1 Materials & sample preparation

The experiments were conducted at Santa Maria using the material and machines present on-site. The supervisor prepared and supplied the samples before performing the experiments. Samples used in the moisture- and mixing speed study were prepared using a proprietary recipe. Due to confidentiality purposes, it will not be disclosed in this study. The samples were placed and sealed in an aluminum bag that prevented light or air from entering. They were then stored in a storage room with a temperature of 17.8 ° C and a relative humidity of 30% in a plastic box.

The in-house samples were named according to the notation below:

Sample notation	
SM	base identifier for in-house sample
xx%	SiO_2 concentration
>	rework done

Table 3: Sample notation for the samples, where rework refers added SiO_2 to reach the final concentration

Rework involves incorporating silicon dioxide into an initial batch to achieve the target SiO_2 concentration. This is a common practice in the food industry to evaluate performance without generating unnecessary waste and excessive production costs. Moreover, the samples denoted direct %-SiO_2 were samples that were freshly produced in the factory, i.e did not undergo any rework.

Sample	**Definition**
SM-1.3%	direct 1.3%
SM-1.5%	direct 1.5%
SM-1.75%	direct 1.75%
SM-1.3%>1.5%	1.3%→1.5% rework once
SM-1.3%>1.5%>1.75%	1.3%→1.5%→1.75% rework twice
SM-1.3%>1.5%	1.3% → 1.75% rework once

Table 4: Sample names for the in-house samples with different levels of anti-caking agent as well as whether they have undergone rework or are directly from the factory

Table 5 denotes the sample names for the samples produced by external suppliers. The samples were named according to the subjective grading received on their flow performance in the factory. All samples have different batches and different flavors, thereby different ingredients. SP-4 and SP-8 have the same flavor but originate from different batches.

Sample name	Grade	Comment
SP-1	6/10	sticks a bit to much to the plates, lots of clumps and attracts moisture.
SP-2	7/10	No problems on the line, sticks a bit to the vibrating plates
SP-3	8/10	Stick well to chips, doesn't stick too much to the plate.
SP-4	8/10	Stick well to chips, doesn't stick too much to the plate.
SP-5	8/10	Stick well to chips, doesn't stick too much to the plate.
SP-6	8/10	Stick well to chips, doesn't stick too much to the plate.
SP-7	8/10	Stick well to chips, doesn't stick too much to the plate.
SP-8	9/10	Stick very well to chips, doesn't stick too much to the plate.

Table 5: Sample names of the suppliers' own cheese seasoning with different grades based on subjective feedback from the factory.

3.2 Rheometric testing of in-house vs external supplier

This section outlines the step-by-step process used to evaluate the rheological behavior of all the samples listed in table 4 and table 5. Each sample was subjected to four standard tests: aeration, shear cell, compressibility, and basic flow energy (BFE) and each test was conducted in duplicate measurements. The order of the test was not fixed as the order did not influence the outcomes.

All the tests began with selecting the appropriate test program from the FT4 software interface. Depending on the test the corresponding vessel and accessories were assembled. For an in-depth methodology of the individual tests, see appendix. Samples were weighed and loaded into the vessel using a funnel and a powder scoop. A brush was used to brush off any excess powder from the vessel and instrument. Once the vessel was secured in place, the FT4 ran the tests including conditioning and subsequent test sequences. Once all test sequences were completed, the data was saved. The same steps were performed for a second replication and the whole process was repeated for all the four rheometric tests.

3.3 Effect of humidity and moisture content on powder flow

To understand the effect of humidity and moisture on the different rheometric properties, three samples were prepared containing three different concentrations of silicon dioxide: 1.3% , 1.5% and 1.75%. Additionally, a reference sample was prepared that contained no silicon dioxide to determine if anti-caking agents posed any effect. All samples were prepared on the same day and stored in aluminum bags for 24 hours prior to conditioning in their respective environment. The following day, half of each sample was put into a 3 L bowl (reference and 1.3% SiO_2) and a 2 L bowl (1.5%, 1.75% SiO_2), then placed in a climate chamber (HPP750eco, Memmert GMBH + co.KG) set to 80% RH and 25 °C. Similar setup was conducted for the winter condition, but the samples were placed on the top shelf in a storage unit with 17.8 ° C and a relative humidity of 30%. See figure below for an illustration of the setup.

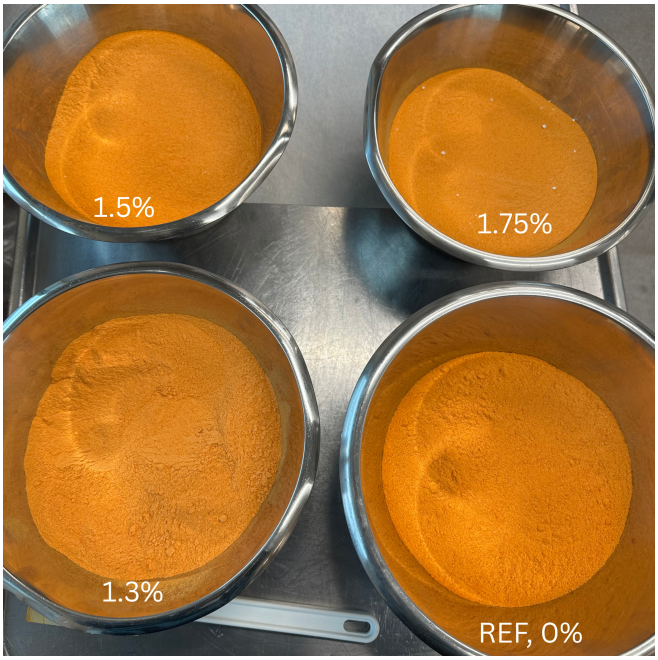

Figure 5: Experimental setup of samples for environmental exposure

In both conditions, the samples were exposed to their respective environment for 3 hours and the samples were stirred after the first 1.5 hour using a spatula before they were placed back into their respective environment. After three hours, half of each sample in each respective condition was placed in an aluminum bag for day 1 testing, and the remaining half was added to a blue plastic bag which is the same bag used for storage in the factory, to simulate real-life storage conditions and incubated for 14 days in respective storage units.

AquaLab 4TE was used for water activity testing and the temperature was configured to 25 °and 17.8 °for summer and winter conditions. 5 g of sample was placed in a small disposable container, ensuring it covered the bottom of the container. The container was then placed inside the instrument, and the lever pulled to the left to begin the measurement. Once the measurement was done, the water activity and temperature was displayed on the screen and recorded. The same procedure was repeated for all samples and each sample was measured thrice.

3.4 Particle morphology

The particle morphology was analyzed by the Danish Technical Institute where 5 samples were sent for analysis. The aim was to analyze the particle size and see if there is any correlation between the methodological characteristics of the samples and their performance. Additionally, investigate if there was any correlation between the results and the findings from the other experiments. Due to the limited number of samples that could be sent, these were the motivation for the sample selection. SP-7 was selected due to being among the top performing sample along with SP-6 and SP-8. SM-1.3% was the original sample with 1.3% SiO_2 and to note if there were any effects of added silicone dioxide, SM-1.75% with a SiO_2 of 1.75% was also sent.

The analysis of the samples was performed with a light microscope (Malvern Morphology G3 microscope) employing 5X and 20X objectives to capture multiple images of a single particle. Each test required 5 mm^2 of sample uniformly spread on the microscopy slide using a Sample Dispersion Unit (SDU).Statistical calculations were applied on a large dataset of about 20 000 particles, where the following parameters were evaluated: circularity, convexity, and elongation. Additionally, the average particle size, referred to as the circular equivalent (CE) diameter, was assessed. The results were presented both on the number distribution (ND) i.e each particle was weighted equally for the average and volume distribution (VD) and each particle was weighed based on their volumes. Simply, small particles have a lower volume in total while larger particles have a higher volume. Depending on the objective, one can evaluate the results by discussing either number distribution or volume distribution. For this study, both will be discussed.

3.5 Shear speed

The last part of the study examined the potential effect of using a high shear mixer in contrast to a low shear mixer. Two 600 g samples were prepared with an in-house cheese chip seasoning containing 1.5% silicon dioxide; one utilized a Moulinex DP8108 (1000 W) high-shear mixer, and the other employed a low-shear mixer from Electrolux. The selected concentration was due to that it performed the best out of all the in-house samples. Once prepared,the samples were then stored in aluminum bags, sealed and stored for testing the consecutive day. Shear cell test and aeration tests were performed using the FT4 powder rheometer. The aeration test was conducted for an air velocity from 0 to 40 mm/s. Additionally, a particle size analysis test was conducted in duplicate measurements for each of the samples. A sieve machine, Prüfsieb JEL 200, was used for the particle size analysis and 4 cylindrical meshes of sizes 0.5mm,0.4mm,0.3mm and 0.15mm placed on top of each other in the descending order, see figure 6. A bottom plate was placed onto the 0.15 mm sieve to collect the remaining powder from the 0.15mm sieve. A plastic sieving cube was placed on each cylindrical sieve except for the bottom plate to help break apart any agglomeration between the powder particles. 50 g of the sample powder was weighed using Mettler Toledo Moisture analyser DBS 60-3 and then loaded onto the top cylindrical sieve (0.5mm) and covered with a top plate. Afterward the tower of sieves was moved to the sieve machine (Prüfsieb JEL 200), locked and the machine set to rotate for 5 minutes.

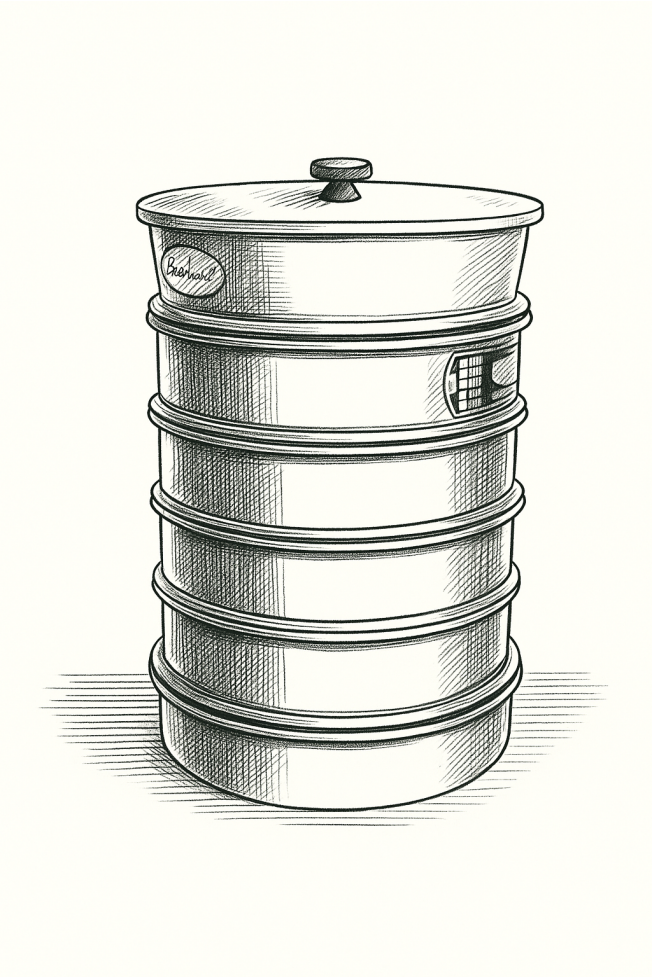

Figure 6: Illustration of sieve analysis set up

After 5 minutes, the tower of sieves were removed from the machine and placed on a counter. Starting with the largest mesh, 0.5 mm, particles retained on the mesh were poured onto a baking paper and then poured on a metal plate. Placing the metal plate on the weighing machine (Mettler Toledo Moisture analyser DBS 60-3), the weight was recorded.The weight retained across each mesh size was documented using the same procedure.

3.6 Data analysis & statistical testing

The results from the FT4 tests were saved in a file that could be opened by the Data Analysis V4 software, a complementary software to the FT4 powder rheometer®. The files for the different tests and samples were imported into the software and graphs were created in the software that could be readily exported. Both the raw data and the average data were exported to an excel document for further analysis. Hypothesis testing was conducted using Datatab, a website that offers a range of statistical tools [40]. One-way ANOVA was employed to determine the statistical significance of the role of silicon dioxide and the effect of environmental conditions.Analogous to the one-way ANOVA, the Mann-Whitney U test was applied to assess the statistical significance of mixing intensity, due to limited replicates and the presumption of non-normally distributed data. Lastly, excel was utilized to create bar plots.

4 Experimental results

The following sections present the results obtained from the different tests, shear cell, aeration, basic flow energy, and compressibility performed using the FT4 Powder Rheometer ®. The sections are divided according to the results obtained from the different studies detailed in section 3.

4.1 Comparative analysis of in-house vs external supplier sample

This section compares the rheological data of the in-house sample (SM-1.3%) and the external supplier samples (SP) obtained from the FT4 tests: shear cell, aeration, compressibility and BFE. SM-1.3% refers to the original in-house sample formulation, which demonstrates poor flow behavior, as noted earlier.

Figure 7 and Figure 8 showcase the aerated energy. The left graph illustrates the data of samples that were tested at an air velocity ranging from 0 to 20 mm/s and the right figure presents samples that were tested at an air velocity ranging from 0 to 40 mm/s. According to both graphs, the best performing sample was SP-8 as expected and least performing SM-1.3%. Most of the external samples exhibit a good curve decline with certain exceptions such as SP-5 where the aerated energy makes a sharp decline at 20 mm/s. Conversely, SP-8 has a sharp incline in aerated energy between 10 mm/s and 20 mm/s which could be attributed to the experimental setup rather than the sample itself. Unlike the external samples, SM-1.3% exhibited poor flow performance, never reaching a state of fluidization at 20 mm/s but obtaining it later at 30 mm/s. The noticeable drop in aerated energy observed in SP-5, alongside an unexpected rise in SP-8, indicates potential threshold effects or experimental inconsistency, highlighting the varied responses to aeration across the samples.

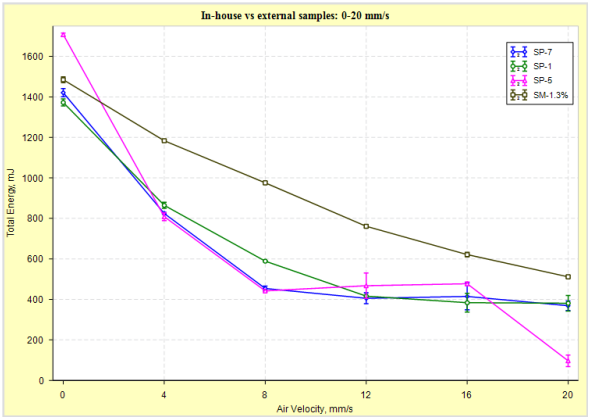

Figure 7: Graph of the suppliers' samples and in-house samples recorded at an air velocity from 0 to 20 mm/s.

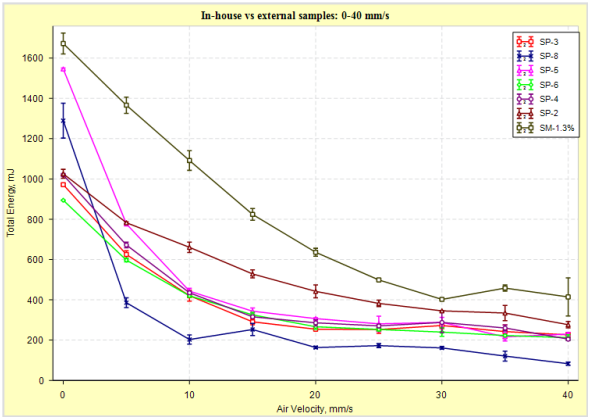

Figure 8: Graph of the suppliers' samples and in-house samples recorded at an air velocity from 0 to 40 mm/s

Table 6 presents the aerated energy at the air velocities 20 and 40 mm/s. SP-8 recorded the lowest aerated energy while SP-2 recorded the highest aerated energy at 20 and 40 mm/s.The same is observed for SM-1.3%. At 20 mm/s, SM-1.3% is the most sensitive to aeration but declines at 40 mm/s. This suggests that air flow forms a channel making it easy for the air to flow past but with increasing air flow, it becomes notably harder to break apart the agglomerates.

Sample	AE_{20}, mJ	AR_{20}	AE_{40}, mJ	AR_{40}
SP-8	163 (±5.85)	7.91 (±0.35)	82.9 (±7.87)	15.6 (±0.435)
SP-3	254 (±4.29)	3.83 (±0.12)	226(±12.1)	4.3 (±0.208)
SP-6	266 (±12.9)	3.36 (±0.23)	212 (±14.1)	4.23(±0.280)
SP-4	286 (±15.4)	3.57 (±0.24)	205 (±6.46)	4.98(±0.124)
SP-5	307 (±3.79)	5.04 (±0.11)	230 (±8.41)	6.74(±0.267)
SP-2	442 (±32.0)	2.32 (±0.17)	277 (±15.7)	3.72(±0.132)
SM-1.3%	636 (±19.8)	11.32 (±0.005)	414 (±94.4)	4.23 (±0.837)
SP-7	369 (±23.6)	3.87 (±0.302)	-	-
SP-1	381(±38.5)	3.64 (±0.413)	-	-

Table 6: Combined aeration test results for external suppliers' samples conducted with a test program with an air velocity ranging from 0 and 20 mm/s. The second test program is conducted at an air velocity ranging from 0 to 40 mm/s.

Sample	Cohesion, kPa	FF	AIF, º	AIF (E), º	AIF (SS), º
SP-8	0.417 (±0.02)	6.693 (±0.27)	29.388 (±1.81)	33.345 (±1.91)	29.418 (±1.58)
SP-4	0.505 (±0.03)	5.621 (±0.30)	29.275 (±0.50)	34.049 (±0.21)	30.035 (±0.27)
SP-7	0.529 (±0.06)	5.350 (±0.48)	33.894 (±0.17)	38.669 (±0.31)	33.964 (±0.48)
SP-3	0.707 (±0.05)	4.280 (±0.19)	33.929 (±0.21)	40.014 (±0.11)	35.859 (±0.31)
SP-2	0.721 (±0.05)	4.032 (±0.18)	29.134 (±0.84)	36.009 (±0.44)	31.326 (±0.16)
SP-6	0.744 (±0.01)	4.107 (±0.01)	34.002 (±0.33)	40.363 (±0.32)	36.106 (±0.33)
SP-1	0.884 (±0.02)	3.384 (±0.06)	32.397 (±0.08)	40.456 (±0.23)	35.236 (±0.15)
SP-5	0.972 (±0.03)	3.107 (±0.03)	32.072 (±0.73)	40.994 (±0.57)	35.452 (±0.19)
SM-1.3%	0.534 (±0.05)	5.432 (±0.55)	32.751 (±0.80)	37.515 (±1.24)	33.454 (±1.01)

Table 7: Shear cell of in-house and external supplier samples.

Shear cell results noted in table 7 further highlights the rheological differences between the samples. Among the samples, SP-8 remains undisputedly the least cohesive in terms of cohesion and across all the other parameters. In contrast to the aeration results, SM-1.3% performs better with a cohesion value of 0.534 kPa which is close to the best performing sample (SP-8) while SP-5 scores the highest in cohesion (0.972 kPa). AIF which defines the powder's general resistance to flow is low for SP-8 and highest for SP-6 but remaining small for SM-1.3%. Under maximum load (AIF(E)), SP-4 exhibits the highest resistance to flow, and SP-6 exhibits high resistance under continuous flow (AIF(SS)). At glance, there is a strong negative correlation between cohesion and flow function, indicating that these two parameters strongly influence one another. Figure 9 demonstrates a strong inverse relationship between the two parameters, with an R-squared value of 0.955 from linear regression, affirming their interdependence.

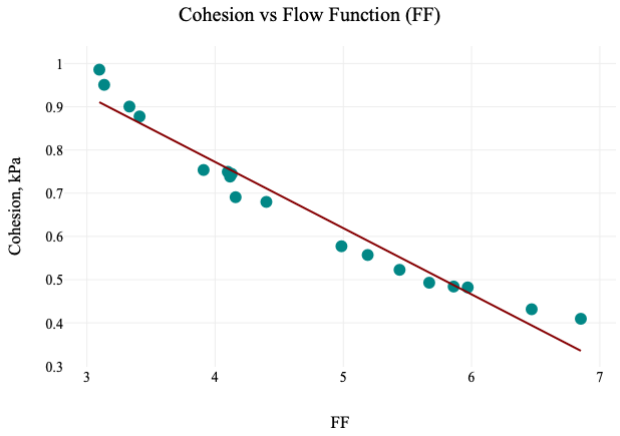

Figure 9: Cohesion vs FF of external supplier and in-house samples.

Sample	CPS, @ 15.0kPa
SP-8	11.8 (±0.438)
SP-4	14.9 (±0.0547)
SP-7	17.5 (±0.339)
SP-6	17.7 (±0.316)
SM-1.3%	19.6 (±0.675)
SP-5	20.5 (±0.336)
SP-2	22.1 (±0.442)
SP-3	24.3 (±3.04)
SP-1	25.3 (±0.689)

Table 8: Compressibility from 0.5 to 15 kPa on suppliers' samples sorted in ascending order according to compressibility percentage at 15.0 kPa.

Table 8 presents the compressibility percentages of the samples subjected to different applied normal stresses from 0.5kPa to 15 kPa. The table is sorted in ascending order according to the compressibility percentages recorded at 15 kPa with visual representation listed in figure 10.

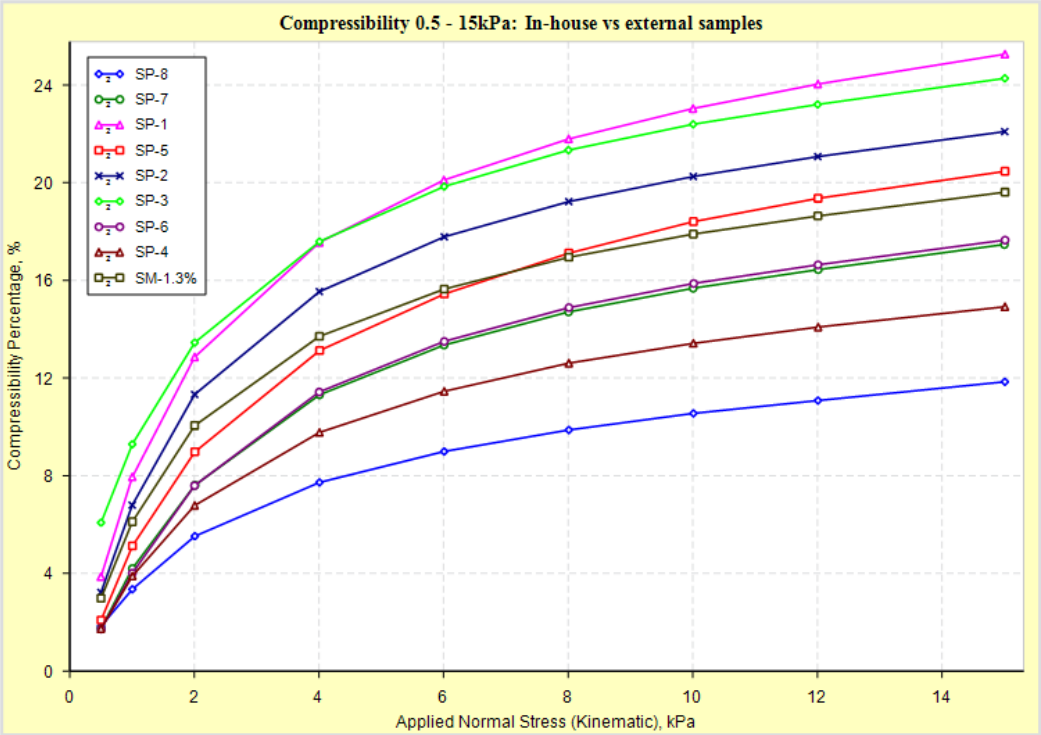

Figure 10: Graph of the suppliers' and in-house samples with the compressibility percentages plotted against the applied normal stresses from 0.5 kPa to 15 kPa.

As demonstrated in the previous two tests, SP-8 has the lowest compressibility with a value of 11.8 %, suggesting poor packing efficiency or differences in the particle shape and size. On the other hand, SP-1 and SP-3 have high compressibility, differing largely from the best performing sample. The compressibility percentage of SM-1.3% is found in-between with a value of 19.6. Findings reveal no clear distinction among the samples and imply other underlying factors such as formulation and processing conditions to influence the results.

Sample	BFE, mJ
SP-6	1021 (±9.57)
SP-3	1150 (±40.3)
SP-2	1154 (±29.8)
SP-7	1227 (±24.8)
SP-4	1264 (±15.6)
SM-1.3%	1280 (±18.5)
SP-1	1287 (±38.5)
SP-8	1321 (±36.5)
SP-5	1512 (±30.7)

Table 9: Basic flow energy (BFE) for SP samples recorded at 100 mm/s

The basic flow energy of the suppliers' samples is presented below organized in ascending order in terms of BFE. SP-6 had the lowest BFE and SP-5 had the highest BFE with a value of 1512 mJ. Interestingly, the best-performing sample demonstrated a relatively high BFE, akin to that of the least performing sample among the suppliers. Variability in the BFE results indicate other underlying factors such as formulation and batch-to-batch variation.

The principal component analysis (PCA) conducted using Datatab reveals 84.4% of the total variance is captured in the first three principal components (PCs), allowing for a meaningful reduction in dimensionality for interpretation. Figure 11 illustrates a visual representation of PC1 and PC2 with a variance of 58.5% and 16.7 % respectively. PC1 distinguishes the samples according to their cohesiveness and shear resistance with cohesion, unconfined yield strength (UYS), major principal stress (MPS) , compressibility (CPS) and flow function (FF) having a strong loading on PC1 .On the other hand, PC2 distinguishes the samples according to aeration with AE_{20} and AR_{20} as key parameters. There is no clear clustering among the samples but rather they are scattered, suggesting that differences in their rheological behavior might be relative and multidimensional. SM-1.3% and SP-8 are positioned far from each other indicating differences in their flow behavior with SM-1.3% being more cohesive as documented in the shear cell results. Similarly, SP-5 is also positioned far from SP-8 and SM-1.3 due to its high cohesiveness as demonstrated in the shear cell- and compressibility test. Interestingly, SP-4 and SP-8 which have the same formulation but different batches are also positioned far from each other along PC1, suggesting a variation in their rheological behavior is found in their cohesiveness and shear resistance. These findings are reflected in earlier results.

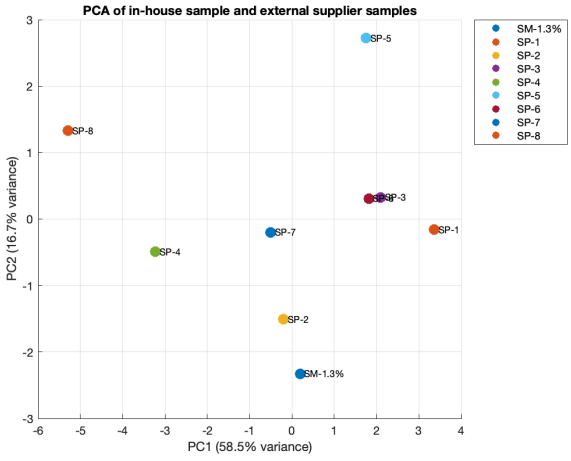

Figure 11: PCA of in-house sample and external supplier samples illustrating PC1 and PC2.

4.2 Rheometric properties: anti-caking agent

Figure 12 and figure 13 depicts the aerated energy for the in-house samples. The left figure contains samples that were measured at an air velocity between 0 and 20 mm/s and the figure to the right compares the samples which have not undergone any rework, i.e direct %-SiO_2 in the samples. As can be observed on figure 13, both SM-1.3% and SM-1.75% were measured at an air velocity extending to 40 mm/s. On the other hand, SM-1.75% was limited to 20 mm/s as with the samples to the left graph. According to the FT4 manual, if the samples had reached a fluidized state at a particular air velocity, no increase in air velocity was necessary. Therefore, it was observed that in figure 12 SM-1.75% and SM-1.3%>1.5% obtained fluidization at 4 mm/s whilst SM-1.3%>1.5% and SM-1.3%>1.5%>1.75% reached fluidization at approximately 12 mm/s. Similarly in figure 13, SM-1.5% appeared to be fluidised at 20 mm/s and as for 1.3% this was observed at 30 mm/s.

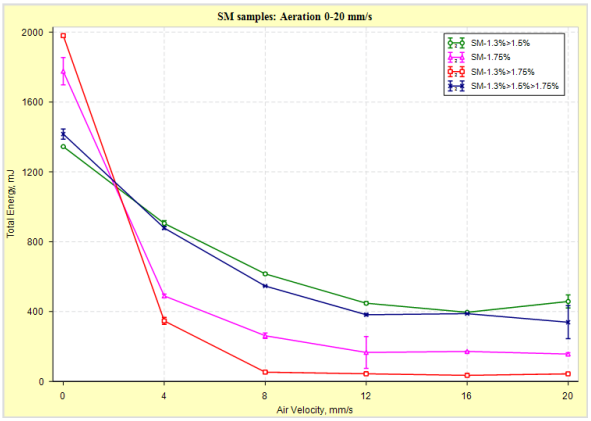

Figure 12: Aerated energy for SM samples containing 1.3%, 1.5% and 1.75% silicon dioxide, tested at an air velocity from 0-20 mm/s.

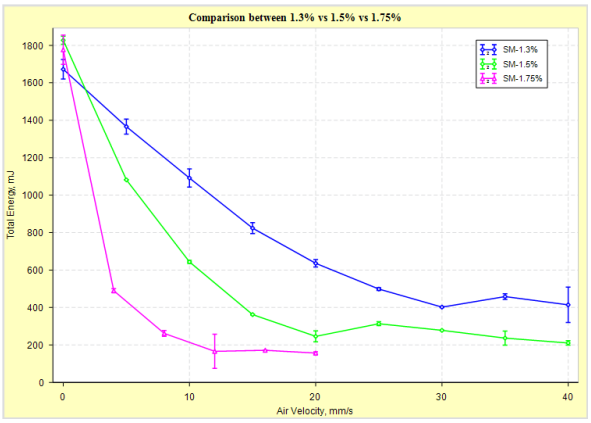

Figure 13: Comparison between 1.3 vs 1.5 vs 1.75 $SiO_2$from the aeration test.

Sample	AE_{20}, mJ	AR_{20}	AE_{40}, mJ	AR_{40}
SM-1.3%>1.75%	43.3 (±0.408)	45.8 (±0.226)	-	-
SM-1.75%	157 (±7.07)	11.3 (±0.0104)	-	-
SM-1.3%>1.5%>1.75%	339 (±94.6)	4.51 (±1.17)	-	-
SM-1.3%>1.5%	458 (±37.8)	2.96 (±0.243)	-	-
SM-1.5%	246 (±29.5)	5.84 (±0.26)	211 (±12.0)	8.71 (±0.598)
SM-1.3%	636 (±19.8)	11.32 (±0.005)	414 (±94.4)	4.23 (±0.837)

Table 10: Aerated energy for in-house samples that have undergone either rework or are direct concentrations. First four samples are measured with an air velocity ranging from 0-20 mm/s. The remaining two have been evaluated at an air velocity ranging from 0-40 mm/s.

Table 10 presents the aerated energy recorded at an air velocity of 20 mm/s and 40 mm/s. Samples are ranked according to aerated energy at 20 mm/s except for the last two samples. According to Table 2, SM-1.3%>1.75% had the minimal aerated energy at 20 mm/s, with an AR_{20} of 45.8, indicating high aerability and aeration sensitivity. Conversely, SM-1.3% exhibited the greatest aerated energy at both 20 mm/s and 40 mm/s, indicating its high cohesiveness. However, in terms of sensitivity SM-1.3% has a similar sensitivity to aeration at 20 mm/s as SM-1.75% which could be due to channels forming through the powder in SM-1.3% as discussed in section 2. Additionally, data values have low deviation, highlighting the accuracy of the FT4 powder rheometer®.

A comparison of the samples with direct SiO_2 is listed on table 11, suggesting a negative correlation between level of silicon dioxide and aerated energy. Statistical analysis demonstrates that silicon dioxide influences the aerated energy at a velocity of 20 mm/s with a p-value less than 0.001, supporting the findings.

Sample	AE_{20}	AR_{20}	AE_{40}, mJ	AR_{40}
SM-1.75%	157 (±7.07)	11.3 (±0.0104)	-	-
SM-1.5%	246 (±29.5)	5.84 (±0.26)	211 (±12.0)	8.71 (±0.598)
SM-1.3%	636 (±19.8)	11.32 (±0.005)	414 (±94.4)	4.23 (±0.837)

Table 11: Aerated energy for SM samples containing 1.3%, 1.5% and 1.75% silicon dioxide, tested at an air velocity from 0-20 mm/s and 0-40 mm/s. Sorted according to aerated energy recorded at 20 mm/s.

	Sum of Squares	df	Mean Square	F	p
%-SiO2	259842.33	2	129921.17	147.72	.001
Residual	2638.5	3	879.5		
Total	262480.83	5			

Table 12: One-way ANOVA analysis of the effect of silicon dioxide on the aerated energy recorded at an air velocity of 20 mm/s.

The table below illustrates the results from the shear cell results for the samples with different levels of anti-caking agent, ranked according to the cohesion values. Notably, SM-1.3%>1.75% with a final concentration of 1.75% SiO_2 had the lowest cohesion value of 0.279 kPa as opposed to SM-1.3%>1.5% that had a final SiO_2 of 1.5% with a cohesion value of 0.621 kPa. All the samples according to Jenike's flowability classification lie above 4, implying they are all free-flowing with SM-1.75% scoring the highest in FF with SM-1.3%>1.5%>1.75% and SM-1.3%>1.5% recording low values in FF. In terms of the general resistance to flow as depicted by AIF, SM-1.75% had the highest resistance but scoring low when evaluated during dynamic conditions (AIF (E)). Conversely, this is observed during continuous flow conditions (AIF(SS)) where the angle remains relatively low in comparison to the other samples. This implies that the AIF might be influenced by particle shape and size as SM-1.75% has a higher concentration of SiO_2 but during flow, it breaks apart easily and remains free-flowing.

Sample	Cohesion, kPa	FF	AIF, º	AIF (E), º	AIF (SS), º
SM-1.3%>1.75%	0.279 (±0)	9.945 (±0.11)	33.127 (±0.422)	35.632 (±0.44)	31.945 (±0.42)
SM-1.75%	0.315 (±0.06)	8.856 (±1.49)	34.005 (±0.95)	36.803 (±0.44)	32.919 (±0.373)
SM-1.5%	0.441 (±0)	6.525 (±0.03)	33.545 (±0.62)	37.424 (±0.57)	33.598 (±0.54)
SM-1.3%	0.534 (±0.05)	5.432 (±0.55)	32.751 (±0.80)	37.515 (±1.24)	33.454 (±1.01)
SM-1.3%>1.5%>1.75%	0.600 (±0.04)	4.889 (±0.26)	31.967 (±0.55)	37.356 (±0.20)	33.300 (±0.11)
SM-1.3%>1.5%	0.621 (±0.02)	4.662 (±0.1)	32.250 (±0.21)	37.905 (±0.33)	33.372 (±0.27)

Table 13: Shear cell results of the SM samples with different levels of anti-caking agent, ranked according to cohesion in ascending order.

The table suggests,there is a strong negative correlation between cohesion and the flow function (FF), where it can be noted that as the cohesion value increases, the flow function decreases, suggesting a possible relationship between cohesion and FF. This is also illustrated in the figure below. The R-squared value is high (0.9859) suggesting a high correlation between cohesion and the flow function.

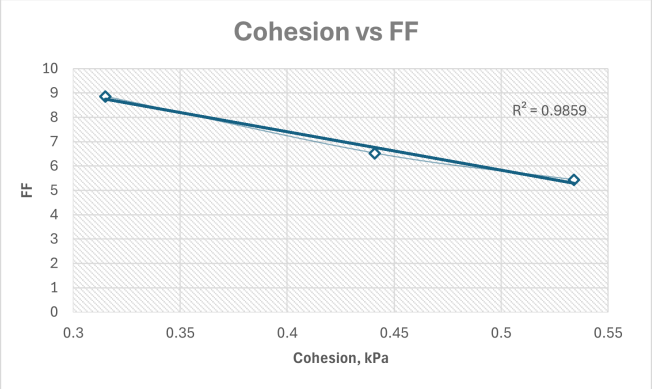

Figure 14: Plot of the cohesion values vs FF for 1.3%, 1.5% and 1.75% samples

Conducting a single ANOVA test on the different samples (SM-xx) with direct %-SiO_2 against the cohesion reveals there is a statistical significance, see table 14. The F-statistic with a value of 11.13 is greater than the F_{crit}, and the p-value is also significantly smaller than 0.05 with a value of 0.041. Therefore, the null hypothesis is rejected; there is no difference in means between at least two groups. Instead, the alternative hypothesis, which states that there is a difference between at least two mean groups, is accepted. However,one-way ANOVA on the %-SiO_2 and flow function revealed no statistical significance, hence the null hypothesis was rejected. See table 15.

	Sum of Squares	**df**	**Mean Square**	**F**	**p**
%-SiO2	0.04	2	0.02	11.13	.041
Residual	0.01	3	0		
Total	0.05	5			

Table 14: One-way ANOVA analysis of the effect of silicon dioxide on the cohesion.

	Sum of Squares	**df**	**Mean Square**	**F**	**p**
%-SiO2	12.78	2	6.39	7.51	.068
Residual	2.55	3	0.85		
Total	15.33	5			

Table 15: One-way ANOVA analysis of the effect of silicon dioxide on the flow function.

Sample	**CPS, % @ 15.0kPa**
SM-1.75%	13.1 (±0.178)
SM-1.5%	16.3 (±0.816)
SM-1.3%>1.5%	18.2 (±0.551)
SM-1.3%>1.5%>1.75%	18.6 (±0.625)
SM-1.3%	19.6 (±0.675)
SM-1.3%>1.75%	9.24 (±0.350)

Table 16: Compressibility for SM samples at different pressures, sorted according to least compressibility percentage to highest compressibility at 15 kPa.

Table 16 illustrates the compressibility of the different samples that have been subjected to a compression of 15.0 kPa. The samples are sorted according to least to highest compressibility. SM-1.3%>1.75% had the lowest compressibility whereas SM-1.3% had the highest compressibility. It can be noted that there is negative correlation SiO_2 between %- SiO_2 and CPS where the less silicon dioxide is present, the higher the compressibility. Figure 15 and figure 16 depicts the compressibility graphs for the different in-house samples with the applied normal

stress plotted against the compressibility percentage. As previously mentioned, the blue graph (SM-1.3 %) had the highest compressibility in both figures. The lowest in figure 15 was the pink graph (SM-1.35 % > 1.75%) but in figure 16 it was the green graph (SM-1.75 %). From this observation, it can be inferred that both samples contain a final concentration of 1.75% SiO_2 suggesting possible correlation between SiO_2 and the compressibility percentage.

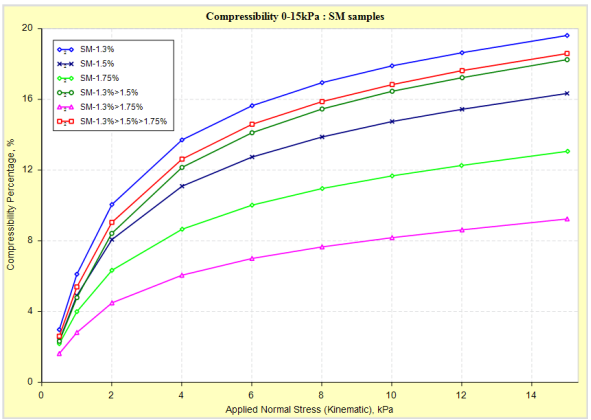

Figure 15: Graph of the in-house samples with the compressibility percentages plotted against the applied normal stresses from 0.5 kPa to 15 kPa.

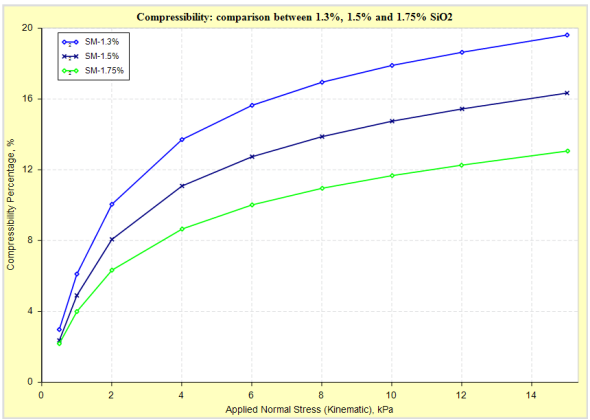

Figure 16: Comparison of the compressibility percentages recorded for the direct %-SiO_2,1.3 vs 1.5 vs 1.75 SiO_2

Furthermore, in the right figure, SM-1.5% has a compressibility percentage in between the baseline and maximum SiO_2. This can be observed in figure 15 which sample SM-1.3%> 1.5% with the same final concentration although has undergone rework, the compressibility percentages are close to one another.

	Sum of Squares	df	Mean Square	F	p
%-SiO2	42.9	2	21.45	26.05	.013
Residual	2.47	3	0.82		
Total	45.37	5			

Table 17: One-way ANOVA analysis of the effect of silicon dioxide on compressibility

One-way ANOVA analysis displayed on table 17 suggests silicon dioxide influences the compressibility of the samples with an F-value of 26.05 and a p-value of 0.013 at a 5% significance level.

Sample	BFE, mJ
SM-1.3%	1280 (±18.5)
SM-1.3%>1.5%	1301 (±0.372)
SM-1.3%>1.5%>1.75%	1335 (±47.5)
SM-1.3%>1.75%	1773 (±49.8)
SM-1.5%	1824 (±29.2)
SM-1.75%	1864 (±21.5)

Table 18: Basic flow energy of SM samples recorded at 100mm/s.

Table 18 presents the basic flow energy (BFE, mJ) for the in-house samples recorded at 100 mm/s and sorted in ascending order. SM-1.3 % scored the lowest of basic flow energy and SM-1.75 % scored the highest on basic flow energy. A notable trend is observed regarding the influence of silicon dioxide, where increasing levels correspond to an increase in BFE.

4.3 Rheometric properties: humidity vs anti-caking agent

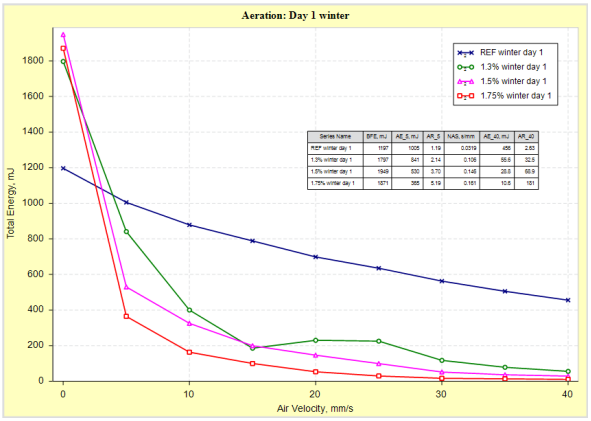

Figure 17: Aerated energy for samples subjected to winter conditions that tested at an air velocity from 0-24 mm/s at day 1.

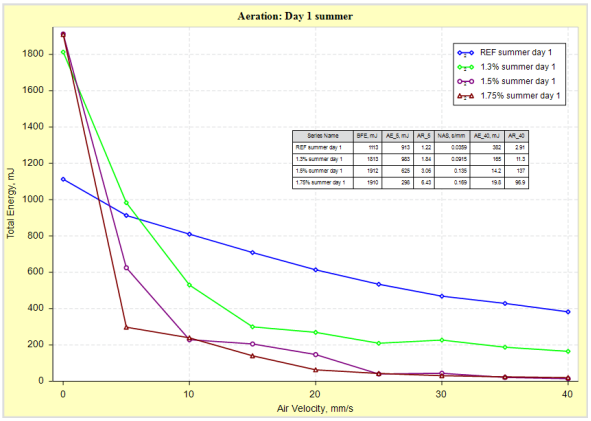

Figure 18: Aerated energy for samples subjected to summer conditions that tested at an air velocity from 0-24 mm/s at day 1.

The figures above present the aeration results of the samples subjected to the two conditions, summer and winter measured on day 1. In both graphs, the reference samples exhibit large aerated energy at 40 mm/s and a trend can be observed for samples between level of silicon dioxide and aerated energy. In general but with a few discrepancies, it can be noted that the aerated energy at 40 mm/s is higher for samples subjected to summer condition as opposed to the winter samples.

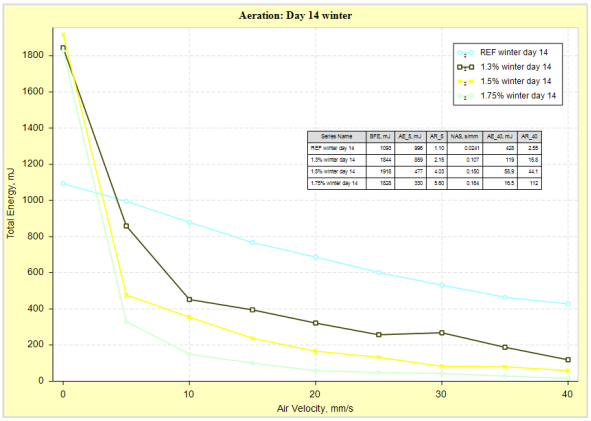

Figure 19: Aerated energy for samples subjected to winter conditions that tested at an air velocity from 0-24 mm/s at day 14.

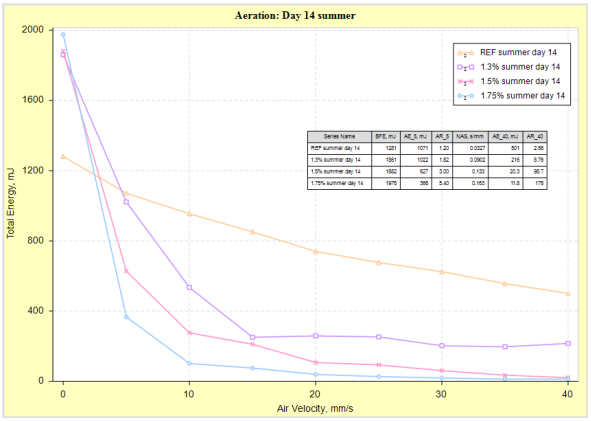

Figure 20: Aerated energy for samples subjected to summer conditions that tested at an air velocity from 0-24 mm/s at day 1.

Figure 19 and figure 20 present the aeration results at day 14 for the samples subjected to winter and summer conditions. Conversely to the figures above, the reference samples had higher aerated energy at 40 mm/s. Moreover, there is a negative correlation between the level of silicon dioxide and the aerated energy.

The table below presents the aeration ratio (AR_{40}) and aerated energy (AE_{40}) values for samples subjected to two different conditions (summer and winter) with varying silicon dioxide concentration. There is a clear trend with increased SiO_2 which correlates with higher (AR_{40}) and lower (AE_{40}), indicating improved flow and reduced cohesiveness, especially notable for the 1.75% samples across all conditions. Samples subjected to summer conditions, generally exhibit lower (AR_{40}) and higher (AE_{40}) values than samples subjected to winter conditions, especially on day 1, demonstrating increased moisture sensitivity and a more pronounced increase in flow resistance. After 14 days, findings reveal an increase in (AE_{40}) across all samples with REF samples maintaining poor aeration

sensitivity. Interestingly, the 1.5% sample subjected to summer conditions, shows increased (AE_{40}) despite high (AR_{40}), suggesting some non-linear effects, possibly due to environmental interaction or sample heterogeneity.

Sample	**AR_{40}**	**AE_{40}**
REF winter day 1	2.63 (±0.113)	456 (±3.82)
1.3% winter day 1	32.5 (±1.8)	55.6 (±4.75)
1.5% winter day 1	68.9 (±8.93)	28.8 (±3.99)
1.75% winter day 1	181 (±24.9)	10.6 (±1.55)
REF summer day 1	2.91 (±0.025)	382 (±6.76)
1.3% summer day 1	11.3 (±1.76)	165 (±26.7)
1.5% summer day 1	137 (±17.7)	14.2 (±1.37)
1.75% summer day 1	96.9 (±5.84)	19.8 (±1.4)
REF winter day 14	2.55 (±0.125)	428 (±16.4)
1.3% winter day 14	15.8 (±2.14)	119 (±15.2)
1.5% winter day 14	44.1 (±22.7)	58.9 (±29.9)
1.75% winter day 14	112 (±7.89)	16.5 (±1.58)
REF summer day 14	2.56 (±0.036)	501 (±13.3)
1.3% summer day 14	8.76 (±0.924)	216 (±30.1)
1.5% summer day 14	95.7 (±16.5)	20.3 (±3.92)
1.75% summer day 14	176 (±38.9)	11.8 (±2.57)

Table 19: Summarised aeration test data for samples subjected to winter and summer conditions measured at day 1 and day 14 at air velocity ranging from 0 to 40 mm/s.

The shear cell data presented in table 20 reveals reduced cohesion with increasing silicon dioxide across all conditions and time points. Correspondingly, these samples show high flow function (FF) values, indicating high FF value at 19.544 (1.75% winter day 1) and 13.867 (1.75% summer day 1), far surpassing the reference samples. The angle of internal friction (AIF) and its derivatives (AIF(E) and AIF(SS)) exhibit minor variations across conditions. Notably for AIF(E), the reference samples have higher values in both conditions, suggesting increased flow resistance at maximum loading. Furthermore, the reference samples maintain a high flow resistance under continuous flow (AIF(SS)), suggesting the presence of interparticle forces. Samples exposed to higher humidity (80% RH) and longer storage (day 14) generally exhibit increased cohesion and reduced FF, especially for reference samples.

Sample	Cohesion, kPa	FF	AIF, º	AIF (E), º	AIF (SS), º
REF summer day 1	0.900	3.325	35.404	43.315	37.512
REF winter day 1	1.190	2.736	33.043	43.262	38.148
1.3% winter day 1	0.330	8.505	35.152	38.028	34.064
1.5% winter day 1	0.319	8.970	33.781	36.548	33.191
1.75% winter day 1	0.142	19.544	33.551	34.796	31.682
1.3% summer day 1	0.414	6.865	34.522	38.154	34.141
1.5% summer day 1	0.301	9.274	34.633	37.279	33.466
1.75% summer day 1	0.199	13.867	33.960	35.720	32.231
REF summer day 14	1.233	2.679	33.240	43.688	38.659
REF winter day 14	0.998	3.057	34.516	43.325	37.583
1.3% winter day 14	0.363	7.811	33.912	37.106	33.302
1.5% winter day 14	0.325	8.774	33.387	36.233	32.811
1.75% winter day 14	0.242	11.836	31.898	34.020	31.196
1.3% summer day 14	0.420	6.724	34.527	38.239	34.018
1.5% summer day 14	0.321	8.686	34.942	37.764	33.735
1.75% summer day 14	0.257	10.811	35.368	37.603	33.825

Table 20: Summarised shear cell test data for samples subjected to winter and summer conditions measured at day 1 and day 14.

Figure 21 and figure 22 shows the water activity for the winter and summer samples recorded at day 1 and day 14. Overall, all the summer samples recorded higher water activity in comparison to the winter samples. There is no observable trend in terms of level of silicon dioxide and water activity as water activity was the highest for the 1.3 % sample. Figure 22 which depicts the water activity for the samples at day 14 also exhibits a similar pattern in relation to the summer samples. However, reference sample subjected to winter conditions had a higher water activity as opposed to its equivalent in the summer condition. The amount of water activity appears to decrease with increasing %-SiO_2, however considering both 1.50 % and 1.75 % lie on the same line on the graph, it is not statistically significant.

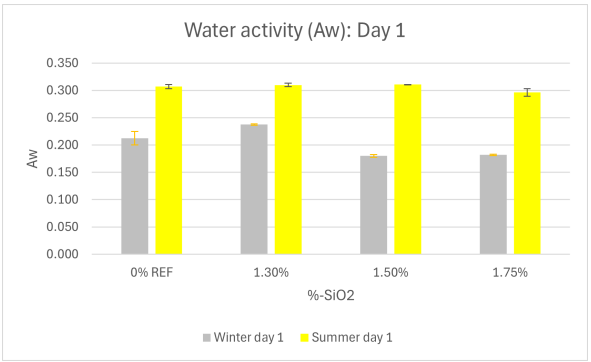

Figure 21: Plot of the measured (A_w) at day 1 for samples subjected to both winter and summer conditions

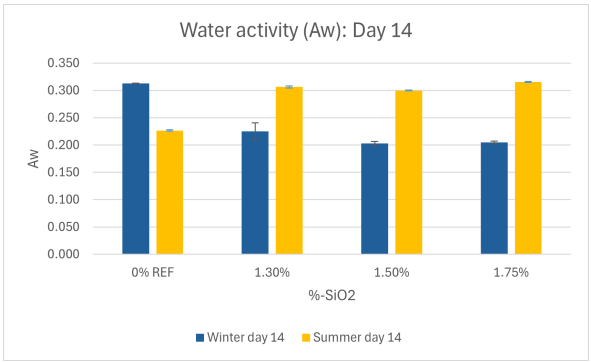

Figure 22: Plot of the measured (A_w) at day 14 for samples subjected to both winter and summer conditions

The below figures organize the samples according to summer and winter conditions. As for figure 23, the water activity for the reference sample appears to be significantly larger on day 1 as opposed to day 14. Notably, the water activity for the other samples appears to be somewhat similar with small decreases in water activity for

the samples 1.3 % and 1.5% and a small increase for sample 1.75 % recorded at day 14. The right figure with the water activity for the winter samples has the opposite trend. The reference sample at day 14 is the highest among all samples. Additionally, there is a trend in increased water activity for day 14 samples and increasing silicon dioxide expect for sample 1.3 %. However, this can be disregarded as insignificant due to the standard deviation.

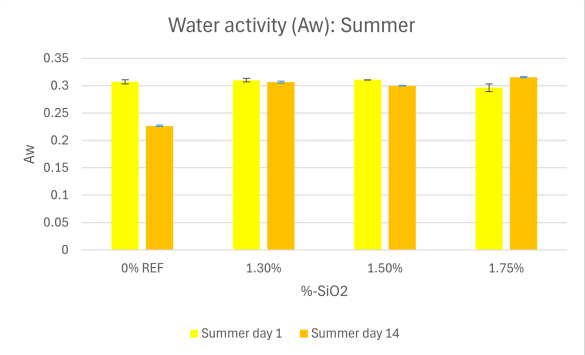

Figure 23: Plot of the measured (A_w)for samples subjected to summer conditions

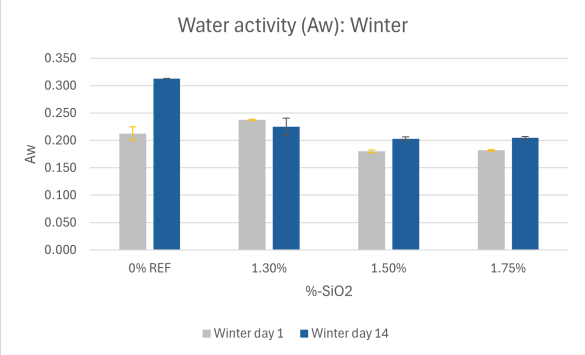

Figure 24: Plot of the measured (A_w)for samples subjected to winter conditions

The one-way ANOVA analyses for samples subjected to winter conditions at day 1, table 29, and day 14, table 22, revealed statistically significant differences in flow behavior across the tested formulations. On day 1, the F-value of 54.88 ($p<0.001$) indicates a strong effect of sample composition. By day 14, this effect intensified, with an F-value of 121.1 ($p<0.001$), suggesting that storage under winter conditions further differentiates the samples. These results confirm that formulation differences significantly influence rheological behavior over time. Conversely, the one-way ANOVA results for samples subjected to summer conditions indicate significant effects of relative humidity on flow behavior, see appendix. At day 1, the F-value of 7.15 ($p=0.012$) reveals moderate differences between samples. However, by day 14, these differences became markedly more pronounced, as shown by a dramatic increase in the F-value to 3592.7 ($p<0.001$). This suggests that prolonged exposure to summer-like conditions heightens differences in cohesion, highlighting the importance of environmental resilience in seasoning formulation.

	Sum of Squares	df	Mean Square	F	p
Sample	0.01	3	0	54.88	<.001
Residual	0	8	0		
Total	0.01	11			

Table 21: One way ANOVA for samples subjected to winter conditions tested at day 1

	Sum of Squares	df	Mean Square	F	p
Sample	0.02	3	0.01	121.1	<.001
Residual	0	8	0		
Total	0.02	11			

Table 22: One way ANOVA for samples subjected to winter conditions tested day 14

Conclusively, the shear cell data correlates well with the values gained in the water activity tests, i.e moisture leads to an increase in cohesion.

4.4 Particle morphology

Table 23 illustrates the average values from four key morphological parameters: diameter, circularity, convexity and elongation. Diameter indicates the size of the particle, while circularity assesses its sphericity. Convexity evaluates the particle's smoothness,and elongation determines how much the particle shape deviates in its width. The means are presented in volume distribution (VD) and number distribution (ND) where volume distribution weights particles by their volume, emphasizing larger particles, while number distribution gives equal weight to all particles, regardless of size, focusing on count and uniformity. Most of the samples are comparable to one another except for SP-6 and SP-8 as there is a large variation between the measurements. See appendix for raw data.

	Diameter					**Circularity**		**Convexity**		**Elongation**	
	ND mean	VD mean	dn(0.1)	dn(0.5)	dn(0.9)	ND mean	VD mean	ND mean	VD mean	ND mean	VD mean
SP-7	15.83	146.3	2.09	10.83	33.58	0.851	0.892	0.98	0.982	0.216	0.487
SP-6	20.27	173.9	2.32	15.52	39.49	0.848	0.889	0.981	0.984	0.232	0.466
SM-1.3%	27.16	189.8	4.77	20.8	52.56	0.831	0.877	0.973	0.976	0.231	0.476
SP-8	9.23	153.5	3.55	7.07	14.94	0.904	0.921	0.988	0.989	0.164	0.383
SM-1.75%	11.06	170.9	2.36	7.94	20.3	0.849	0.891	0.973	0.978	0.196	0.445

Table 23: Morphological characteristics combined - The mean value for particle size, circularity, elongation and convexity according to both number distribution (ND) and volume distribution (VD), furthermore for the particle size the percentiles d(0.1),d(0.5), d(0.9) based on ND is given.

In terms of particle size, SM-1.3 % recorded a significantly higher mean (ND) with a value of 27.16 μm. Conversely, SM-1.3% shows high d(x) values of 4.77, 20.8, and 52.56μm respectively, indicating that many particles were relatively large, resulting in a broader particle size distribution (PSD). On the other hand, SP-8 which exhibited good flow, demonstrates a significantly smaller mean in particle size (ND) with a value of 9.23 μm. The d(x) values, indicate a narrow PSD with a more homogeneous number distribution of smaller particles as noted for samples, SP-7 and SP-6. Additionally, mean values (ND & VD) for SM-1.75% reveal the sample had a smaller diameter with a narrow size distribution. These findings are visually corroborated by exemplary particle size distribution curves shown in figure 25 and figure 26 for SM-1.3% and SM-1.75%.

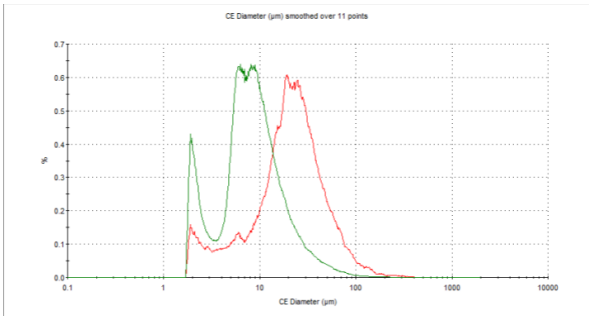

Figure 25: Particle size distribution of SM-1.3(green) and SM-1.75(red) based on the number distribution.

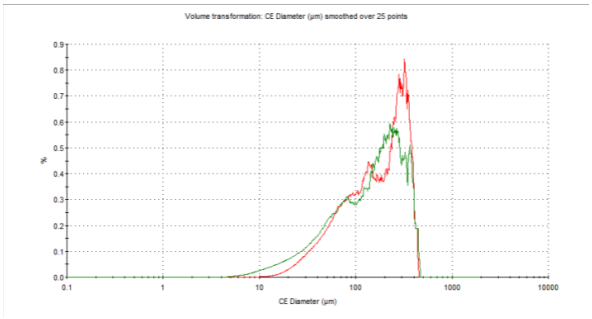

Figure 26: Particle size distribution of SM-1.3(green) and SM-1.75(red) based on the volume distribution (VD).

Figure 25 which presents the PSD based on number distribution, demonstrates a broader and bimodal distribution, suggesting multiple particle populations and increased variability for SM-1.3%(green curve). SM-1.75% (red curve), on the hand, exhibits a single peak, suggesting uniform size and narrow particle size distribution. Figure 26 which is based on the volume distribution further reinforces this observation as SM-1.3% demonstrates a broader distribution skewed towards larger particles by volume. Similarly, SM-1.75% maintains a tighter volume distribution with less variability.

Among the samples, SP-8 exhibited the greatest resemblance to a perfect circle, despite generally high circularity across the board. SM-1.3% as a poor performing sample, has a mean value of 0.831 in number distribution and a mean value of 0.877 in volume distribution. In comparison, SM-1.75% has a slightly higher mean value both in ND and VD, implying a possible correlation between SiO_2 and circularity. Furthermore, the convexity values are highest for SP-8 both on a number- (0.988) and volume distribution (0.989), suggesting the surface of the particles is smoother in surface texture. As for SM-1.3%, convexity values (ND) are similar to SM-1.75%(ND) which might suggest both samples have a similar surface texture. However, detailed analysis using Morphology software reveals variability between the samples as displayed in figure 27.

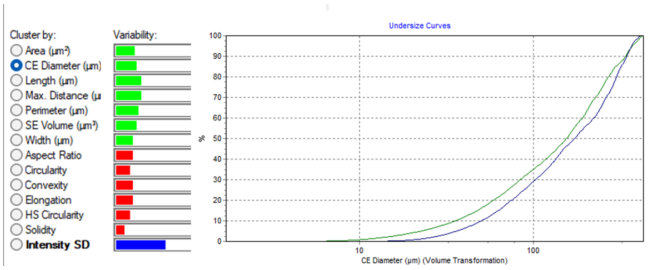

Figure 27: Undersize graph for the convexity of SM-1.3 % (blue) and SM-1.75 % (green).

The graph illustrates the cumulative percentage of particles with a given convexity or lower. The green curve (SM-1.75%) has a steeper initial rise, indicating many particles have a low convexity whereas the blue curve (SM-1.3%) which has a delayed rise, indicates most particles are smoother with a high convexity. Based on this detailed analysis, SM-1.75% appears to have a rougher surface texture in comparison to SM-1.3%. Similar analysis done on all samples reveal their variability in terms of convexity as demonstrated in figure 28

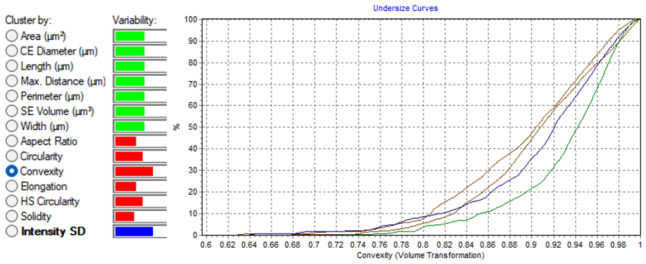

Figure 28: Undersize curves describing the convexity for all the samples.

SP-7 and SP-6, shown in green and blue, respectively, demonstrate the highest variability in convexity among the samples. Conversely, the brown curves represent the other curves, signifying insufficient variability to differentiate the samples. As illustrated, both SP-7(green) has a steep curve, indicating that most samples have high convexity. The steep also suggest high uniformity in surface smoothness i.e. low variability. SP-6, which is slightly to the left of the green curve also indicates relatively high convexity though somewhat more variability in surface smoothness.

4.5 Mixing intensity

The results obtained from the particle sieve analysis are displayed in figure 29 and figure 30. The percentages are calculated as a fraction of the recorded weight retained at the respective mesh size over the total weight from all mesh sizes.

$$\text{Percentage at x mm mesh} = \left(\frac{W_{mm}}{W_{0.5} + W_{0.4} + W_{0.3} + W_{0.15} + W_{<0.15}} \right) \times 100 \tag{1}$$

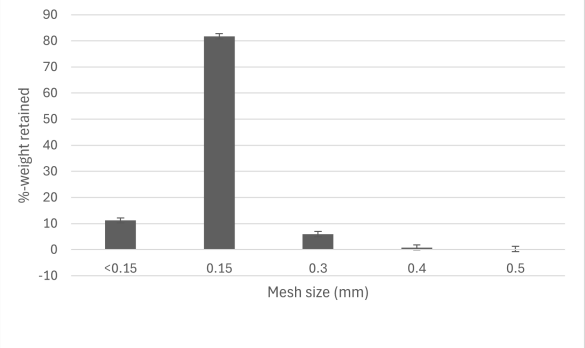

Figure 29: Bar plot of %-weight retained at each mesh size for sample produced using a low shear mixer.

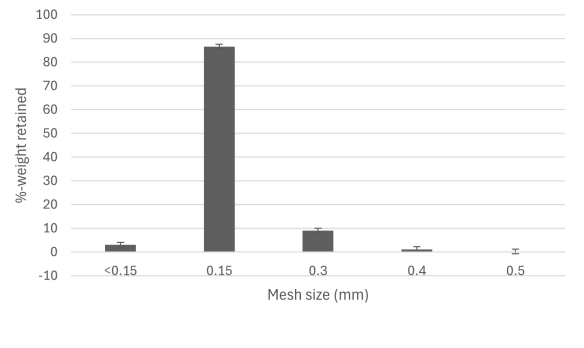

Figure 30: Bar plot of %-weight retained at each mesh size for sample produced using a low shear mixer

Both samples prepared with the different mixer types recorded the same weight at each mesh size, suggesting no difference in particle size distribution. In comparison to the weight retained at the bottom plate, more weight was retained for the sample prepared with a low shear mixer than for the high shear. The opposite effect was observed for the high shear mixer in the 0.3 mm mesh size, indicating the presence of agglomerates due to high shear mixing. Statistical test using the Mann-Whitney U test in table 24 reveals no statistical significance between the two mixing types at a 5% significance level. The null hypothesis which stated there is no difference among the means of the two mixing intensities was therefore not rejected. The alternative hypothesis was that there is a statistical difference. The p-value is 0.917 above the common significance threshold which suggests the result is not significant at the 5% level. The exact p-value is above the asymptotic p-value, also indicating a non significant result at the 5% level. The r-value which denotes the effect size is relatively small, implying the effect of the mixing types is small.

U	**z**	**asymptotic p**	**exact p**	**r**
12	-0.1	.917	1	0.03

Table 24: Mann-Whitney U test for the particle size distribution of samples subjected to low- and high shear mixing.

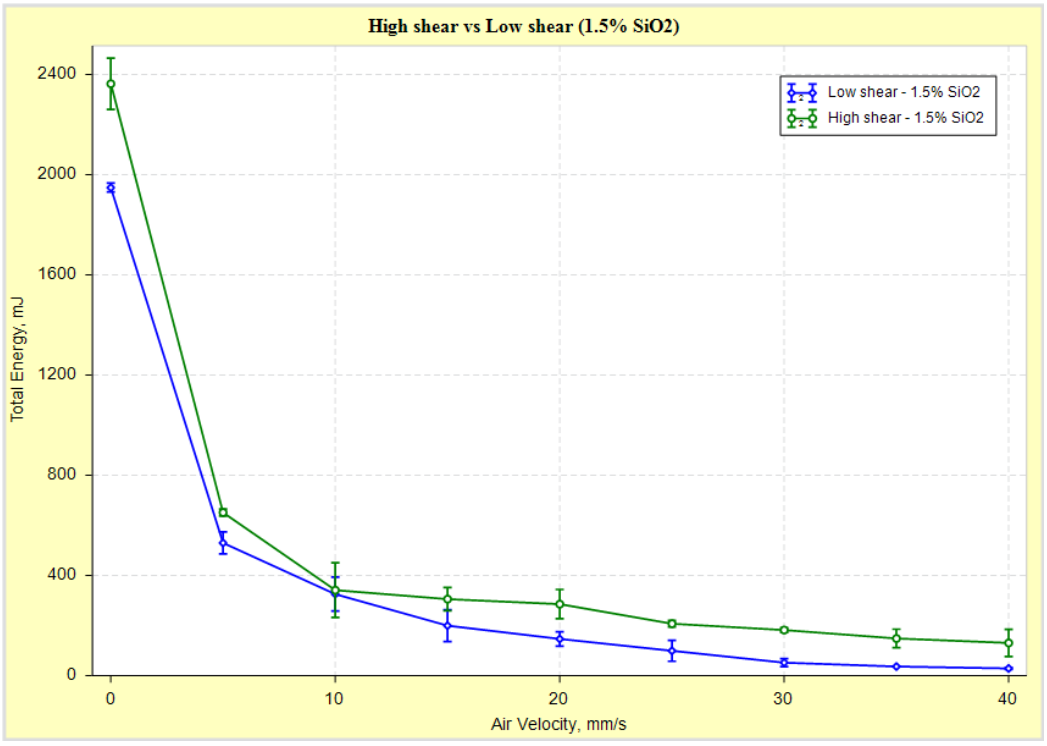

Figure 31: Total energy plotted against air velocity from 0 to 40 mm/s for the low- and high shear samples with 1.5% SiO_2

Figure 25 displays the aerated energy data for samples processed with both high shear and low shear mixer, observed at an air velocity ranging from 0 to 40 mm/s. This graphical representation underscores the points made in the preceding table. In particular, the green curve, representing high shear, consistently exhibits marginally higher aerated energy throughout the experiment.

The table below further displays the quantified aerated energy for the high- and low-shear samples. The high-shear sample had a high basic flow energy with a value of 2363 mJ, while the low-shear sample scored a BFE value of 1949 mJ. Conversely, the high-shear sample had higher aerated energy recorded an air velocity of 40 mm/s with aeration ratio of 21.5. The low shear sample had an aerated energy of 28.8 mJ with an AR value of 68.9, suggesting the sample was susceptible to aeration at higher velocities.

Sample	**BFE, mJ**	**AE_{40}, mJ**	**AR_{40}**
Low shear - 1.5% SiO2	1949 (±17.7)	28.8 (±3.99)	68.9 (±8.93)
High shear - 1.5% SiO2	2363 (±102)	131 (±54.5)	21.5 (±8.19)

Table 25: Aeration results weighted on average for lab scale samples,low shear and high shear with 1.5% SiO2.

Table 26 depicts the results recorded in the shear cell tests for the samples produced using a high shear and low shear mixer. The high shear sample has a higher cohesion value, suggesting increased interparticle forces in comparison to the low shear sample. The angle of internal friction and the angle of internal friction at steady state is lower for the high shear sample but it scores high on the effective angle of internal friction. The ANOVA results for samples subjected to summer conditions indicate significant effects of relative humidity on flow behavior, see appendix.

Sample	Cohesion, kPa	FF	AIF (E),º	AIF (SS), º	AIF, º
Low shear - 1.5% SiO2	0.319	8.970	36.548	33.191	33.781
High shear - 1.5% SiO2	0.446	6.356	37.023	32.888	33.009

Table 26: Shear cell results of the high shear and low shear samples for a test conducted at a pre-consolidation stress of 6kPa.

5 Discussion

The aim of this study was to characterize the flow properties of cheese-based snack seasonings under varying formulation and environmental conditions, using rheometric and morphological analyses. The FT4 powder rheometer® was central to this study, enabling different assessments regarding the flow energy,compressibility and shear behavior of the samples. Furthermore, the morphology of the particles was determined by the Danish Technical Institute, which provided further insights into the physical characteristics that impact flow performance. The discussion that follows, integrates the rheological findings with the morphological data to ultimately identify parameters that could potentially improve seasoning application in the snack food industry.

5.1 Rheological behavior of in-house vs external supplier samples

The main objective of the study was to determine if there were any rheological differences between the in-house samples that were poorly performing to the external suppliers' samples using the FT4 powder rheometer®. As depicted in the PCA plot in figure 11, there was no obvious clustering which indicates that the rheological behavior was influenced by a multitude of factors. This is no surprise however, as powder behavior, as previously stated, is far too complex to be captured by simple groupings, making it resistant to singular classification methods. While the aeration and shear cell tests gave a good indication of the cohesive nature of the samples, the results do not appear to directly translate to their performance in the factory. Notably, SM-1.75% and its rework counterparts (SM-1.3%>1.75%, SM-1.3%>.5%>1.75%) demonstrated aeration results that were most similar to SP-8, the highest-performing external sample. This suggests a degree of convergence in flowability between the optimized in-house formulations and the best external benchmarks. However,in-house samples, including the underperforming SM-1.3%, exhibited lower cohesion values compared to those from external suppliers. These findings suggest that aeration results might not always align with shear cell findings for predicting actual performance, particularly for this instance. One plausible explanation is that the FT4's shear testing, conducted at a preconsolidation stress of 6 kPa, may not reflect the actual stress regimes powders experience in scarfeeders. Thus, while cohesion and FF are useful for benchmarking, they may oversimplify performance outcomes in dynamic environments. Instead, aeration results appear to be better and more relevant predictors for powders exposed to air movement, as is typical during application.

Furthermore, it must be stated the role of formulation in the observed rheological behavior. All samples except SP-8 and SP-4 were derived from different ingredients, adding another factor that could have potentially influenced the results. This introduces a possibility of examining the effects of ingredient interaction with other ingredients, interactions with environment or due to processing effects. In particular, evaluating the role of fat as has been noted previous literature to influence the flowability of powders. A study by Fitzpatrik et. al. found that whole cream milk powder which contains 26% fat content, exhibited greater cohesion in comparison to skim milk powder (1% fat content) [41]. Whole cream milk powder can increase interparticle adhesion by forming capillary bridges or softening particle surfaces, leading to greater cohesion and poorer flowability. This effect might not have been captured by the FT4 powder rheometer®, particularly under standard test conditions that do not simulate heating, vibration, or static build-up present in the factory. Therefore, comparing the samples with different formulations especially when it has been revealed that the in-house samples contained higher fat content in comparison to the external suppliers could help improve the understanding of powder behavior. For a robust comparison, future studies should investigate the role of fat content in the clump formation of the seasonings, particularly by performing tests on only the dairy ingredients.

Further evidence of the role of formulation is observed in the particle morphology analysis. Analysis revealed that SM-1.3% had a larger mean particle diameter overall suggesting greater agglomeration of particles. This conclusion is evidenced through comparison with SM-1.75 which had a relatively smaller diameter although it contained the same formulation but different level of silicon dioxide. The best-performing samples (SP-6, SP-7 and SP-8) had a smaller diameter and narrower particle size distribution (PSD), indicating the role of the physical characteristics on powder flowability. As previously stated in the theoretical background, there are contradictory arguments on the role of a broad versus narrow particle size distribution on flowability. Therefore, the results in this study suggest a broad PSD might be an indicator of poor flowability as observed for SM-1.3%. However, it should be noted that the presence of agglomerates in SM-1.3% might be the cause for a broad PSD and not the size of the individual particles themselves. To add on, a broader PSD affects how efficiently particles pack and that packing efficiency is directly measurable via compressibility. As discussed in the theoretical background, smaller particles can fill the void between large particles thereby improving the packing efficiency. The compressibility

results from this study reveal that a broad PSD does not necessarily lead to better packing or flow. For instance, SM-1.3% demonstrated higher compressibility than SM-1.75% which implies that the presence of fine particles in SM-1.3% may have increased its susceptibility to compaction under load. Particularly by introducing more surface area and thus more interparticle forces such as van der Waals attraction or capillary bridging.

Moving on, the best-performing samples exhibited higher circularity and lower elongation which are traits that have been document in previous studies to improve powder flow. These differences in shape and surface texture likely contributed to the improved flow behavior, as smoother and more spherical particles reduce friction and mechanical interlocking. However, the analysis was conducted with duplicate measurements which is not enough to draw any solid conclusions. While the analysis highlighted the importance of particle size on flowability, convexity results appeared to be similar across all samples, implying they all have a similar surface texture which can be misleading. This was however disproved in the undersize graphs, especially for SM-1.3% and SM-1.75% where the latter sample had a larger fraction of particles with a rougher surface texture. This finding also has implications for understanding powder flow as particles with rougher surfaces have been document to exhibit increased frictional interactions and mechanical interlocking, which results in increased cohesion and reduced flowability. However, SM-1.75% which was slightly more coarse than SM-1.3% performed better in the aeration and shear cell tests. This implies therefore that interpretation of the morphological results should be done with caution i.e not only relying on the mean values but also evaluating the undersize graphs. Future studies should aim to conduct added replicate measures to improve statistical robustness and interpretation.

Conclusively, the findings revealed interesting insights into the complexity of powder behavior and the need for different tests to improve the understanding of the cheese seasonings. Interestingly, the aeration tests provided evidence as helpful predictors of flow performance but the same could not be said for shear cell results, particularly in the context of seasoning adhesion to oil-fried snacks. This further implies and emphasizes the understanding interplay between adhesion and cohesion for snack food coating. Furthermore, morphology analysis revealed that a particle size distribution might be a predictor of powder flowability as well as predicting clump formation in combination with the aeration results.

5.2 Effect of silicon dioxide

This part of the study evaluated the rheometric properties of samples derived from either reworked- or direct concentrations of silicon dioxide. Given industry constraints on time and resources, conducting extensive research is often impractical, making reworks essential for estimation. Here, reworks were necessary to avoid wastage from tonnes of previously produced powders. In this study, reworks of samples with an original concentration of 1.3% SiO_2 demonstrated a decrease in flowability. This was notable in SM-1.3%>1.75% which had overall low aerated energy, reduced cohesion, enhanced flow function, diminished compressibility, and high basic flow energy.In contrast to SM-1.3%>1.5%>1.75%, which possessed an equivalent concentration, the outcomes differed. Differences were more apparent in the aeration and shear cell tests and the underlying differences could be attributed to, for instance, the added mixing time on SM-1.3%>1.5%>1.75% which underwent two reworks. In a study by Eggers et. al, findings revealed that longer mixing times impacted particle size, resulting in larger particles[42]. Although the study evaluated a mixing duration exceeding 48 hours, the results provide insight into the poor performance of the sample reworked twice. Furthermore, differences could also be attributed to the moisture exposure in the twice reworked sample. As previously discussed in section 2, hygroscopic powders are moisture sensitive and readily absorb moisture from the air. In comparison to their direct equivalents, the reworked samples performed poorly except for SM-1.3%>1.75%. The reason for this could be the increased silicon dioxide and the improved dispersion of silicone dioxide. However, if this were the case, this would mean that SM-1.3%>1.5% would exhibit similar behavior. Conclusively, predicting the flowability of rework samples is harder due to a multitude of underlying factors.

To provide a more comprehensive understanding of silicon dioxide's impact on rheometric properties, evaluations of the direct equivalents offer a more thorough insight. It was observed that the addition of silicon dioxide demonstrated a notable difference in flow behavior, indicating a strong correlation between silicon dioxide and flowability. Samples with a final concentration of 1.75 % SiO_2 displayed lower aerated energy, in tests conducted for an air velocity between 0 and 20 mm/s. As shown in table **??**, samples conducted in a test from 0-40 mm/s also revealed that increasing silicon dioxide (SM-1.5%) had lower aerated energy in comparison to 1.3 %. This statement is consistent across all rheometric tests, where increased concentrations of silicon dioxide resulted in lower cohesion values in the shear cell tests, reduced compressibility and higher basic flow energy, suggesting less

cohesive powders with resistance to clumping. In terms of the shear cell test, all the samples the flow function (FF), was above 4 which according to Jenike's classification defines the powders as all easy flowing. However, the FF cannot be used as a predictor in this part of the study because essentially all the samples can be regarded as easy flowing, with no clear distinction between them. It was also observed that elevated levels of silicon dioxide resulted in decreased effective angle of internal friction. The effective angle of internal friction, which indicates the presence of interparticle forces, suggests that added silicon dioxide prevented particles from agglomerating by decreasing the particle-particle interaction. Statistical tests further underscored the effect of silicon dioxide on the different rheometric characteristics. The findings agree with previous literature studies [13] [3].

In terms of humidity, findings revealed humidity to play a role in the flow properties of the cheese seasoning powders produced using a low shear mixer. Powders exposed to summer conditions (25°C, 80 % RH) exhibited increased aerated energy and reduced flowability in comparison to samples subjected to winter conditions (17.8°C, 30 % RH). Figures 12 and 14 illustrate that the reference sample maintained the highest aerated energy at both day 1 and day 14, indicating moisture-induced caking and interparticle adhesion. Notably, the aerated energy decreased with increasing silicon dioxide, displaying a relative resistance to the effects of humidity. For example, SM-1.75 % had a lower aerated energy at 40 mm/s compared to reference and SM-1.3% in both summer and winter agrees with previous studies [13]. However, despite higher SiO_2, the powders still sensitive to moisture over time, thereby emphasizing the importance of formulation and storage. These findings suggest that SiO_2 does initially improve flowability but has limited moisture resistance thus it is important to consider packaging and environmental control in production. Statistical calculations using one-way ANOVA revealed there was statistical significance, implying that the conditions played a role in water activity, further strengthening the results. This observation was made for both day 1 and day 14 samples when comparing the winter samples and summer samples. The ANOVA results also revealed that there was statistical significance in terms of level of SiO_2, indicating the role of silicon dioxide has on powder.

5.2.1 Limitations

While findings reveal there is a significant effect of silicon dioxide on flowability, there are limitations in the study which impacted the results. For instance, in the first part of the study, the tests using the powder rheometer were conducted in duplicate measures. Although the FT4 powder rheometer ® is regarded as accurate and reliable, more data would strengthen the statistical analyses. Duplicate measures were also conducted in the morphology analysis which could also have impacted on the results. This is apparent in the convexity results from the morphology analysis, where both SM-1.3% and 1.75% displayed similar mean values. From a glance, it would appear that the surface roughness for both samples is the same but knowing that there is a higher silicone dioxide concentration means there is more silicon dioxide particles coating the host particles i.e acting as a physical barrier between the particles. This in turn would imply that the surface of the host particles is more coarse hence, the convexity would be lower for SM-1.75%. Fortunately,this was determined from the undersize graph 27 to be accurate. For instance, when exposing the samples to their respective conditions, the winter samples were placed on the top shelf close to a ventilator. The cold air from the ventilator could have caused the samples to absorb more water than expected thus resulting in higher water activity. Furthermore, the samples could have been exposed to a higher relative humidity due to constant movement in the storage room, resulting in an increase in relative humidity from the outside. Additionally, limitations were also found in the humidity tests where the water activity recorded for the reference sample summer day 1 was higher than the water activity recorded at day 14. This discrepancy in results could be attributed to a methodological error. Furthermore, the winter reference sample also exhibited higher water activity at day 14 when compared to the summer reference sample. This could also be attributed to operator error but it could also be due to an methodological error that was observed when measuring the water activity for the winter samples, the machine. Because the winter samples required testing at 17.8 °C, the machine would reject sample therefore requiring the sample to be placed in a freezer for 10 seconds before placed in the machine for measurements. The cold environment in the freezer could have led to the sample absorbing moisture from the air thereby increasing its water activity.

5.3 Effect of mixing intensity

Comparison between samples subjected to two different mixing intensities revealed that there was an observable effect on physical characteristics though it was not statistically significant. The sample that was prepared with a high shear mixer exhibited higher cohesion and aerated energy, likely due to agglomeration of fine particles. As the powders initially have a small particle size, further processing could have potentially resulted to further reduction of the particles. Hertel et al. argue that high shear mixing leads to increased adhesion between particles in turn resulting in the increased cohesion as demonstrated in this study[43]. This observation is also reflected in a similar study that states, the effect of high mixing intensity results in more particle agglomeration with small particles adhering to larger particles and forming a satellite[42]. In addition, findings also revealed that high mixing intensity of fine powders altered the roughness of the surface with particles becoming more damaged and coarser due to particle attrition. It is important to note that this effect presented in the study, was more apparent in combination with longer mixing time. Subsequently, assessing the particle size distribution (PSD) through sieve analysis showed slight variation with different mixers although not a significant change. The Mann-Whitney U test revealed there was no statistical significance in between the mixing types at a significance level of 5%. The null hypothesis was therefore not rejected.

Although the findings indicate that using a high shear mixer could lead to a rather negative impact on the powder flow, it should be considered that the experiment was conducted with duplicate measurements. Future studies could benefit from more robust statistical significance by increasing the number of replicates in the study. The samples were also prepared at different times which could have affected their exposure to humidity and the processing time was different for the low shear in comparison to the high shear. The step-by-step process for preparing the sample using a low shear was also different, requiring longer mixing time and the addition of ingredients was also different. Furthermore, the high shear mixer had a maximum capacity of 250 g of sample per batch whereas the low shear mixer had a capacity of 2500 g. Therefore, these limitations could have an impact on the results and further investigation with more replicates could strengthen the findings. In addition, the implementation of the powders with different mixing conditions in a real-life setting could help evaluate the powder flow performance, especially in regard to adhesion to the tortilla chips. Another limitation was the amount of weight retained at the sieve with a mesh size 0.15 mm. While performing the experiment, it was observed that this particular sieve appeared to be clogged where only the center part was see-through. This could affect the results by only a smaller fraction of the samples were able to move past the 0.15mm sieve. Therefore, repeated experiments with a better sieve would enhance the results and provide more robust data. Lastly, morphological analyses of the samples could provide more understanding on the effects of mixing intensities on the particles. Although this is highlighted in previous studies, the study would benefit from these tests as they would be applied on food powders.

5.4 Industry perspective and practical implications.

From an industrial perspective, the implications of the findings proposed in this study would indicate both a need for increasing silicon dioxide to improve flowability but also a need of reviewing the seasoning formulation. SM-1.3%, which was expected to have a high cohesion value with higher aerated energy compared to the external samples, performed relatively well in the rheometric tests, including shear cell-, compressibility-, and basic flow energy tests. Yet, in the aeration tests it performed poorly which indicates a balancing act between adhesion and cohesion. While addition of flow additives significantly improved its performance, testing of the powder in a real life setting has yet to be done. Observations made in the lab found that increasing the flow additives resulted in increasing dustiness which could reflect negatively in the factory. Therefore, when using the findings to create a design space, flow additive is insufficient for improving the flowability, possible ingredient modifications must be made. In addition, aeration is a crucial test to determine flowability while cohesion might give an indication on how well the seasoning will adhere to itself and to the chips.

Moving on, the company should test the performance of the in-house sample with 1.5% SiO_2 in the factory to evaluate how well the lab-based results reflect real-life. Additionally, evaluate the adhesion of the seasoning to the tortilla chips to test whether improved flowability and decreased cohesion of the in-house sample influences the adhesion. Similarly, testing of the sample produced using a high shear mixer in the factory should also be employed to evaluate whether the small effect that was observed in the lab-based study has a large influence on the flowability. Lastly, in case of persistent poor performance despite the changes, investigation on the fat content and possible change of ingredients should also be explored.

6 Conclusion

The aim of this study was to examine the rheological characteristics of cheese based seasoning powers produced both by Santa Maria AB and their external suppliers. It sought to determine what were the differences exhibited among the samples with a focus on improving their flowability and future handling for industrial snack food coatings. The primary findings demonstrated that the rheological behavior differed between all the samples (in-house vs external suppliers) as observed in the PCA plot and that there are other underlying factors such as formulation and batch-to-variation (SP-4 and SP-8) that affected the observed rheological behavior. Conversely, findings demonstrated that increasing silicon dioxide levels improved flowability up to a threshold of 1.75%. Beyond this, adverse effects such as excessive dusting could occur. The morphological assessment provided evidence of being an indicator for flowability and could be used complementary with rheometric tests to predict powder flowability. Additonally exposure to high relative humidity (80% RH) and prolonged storage (14 days) impacted the flowability.

However, a major key finding and one that should be further investigated was the interplay between adhesion and cohesion. The initial hypothesis was that the in-house sample (SM-1.3%) which was deemed to have poor flowability would exhibit cohesive behavior in the rheometric tests especially the shear cell test. While it did for three of the four tests, a surprising observation was noted when the cohesion values for the in-house samples were lower than a majority of the external supplier samples and had a cohesion value close to the best performing (SP-8). To test the validity of the interplay between adhesion and cohesion, future studies should employ real life testing in the factory with SM-1.5% to see whether that improved its flowability but also if it affected it adhesion to chips.

To build on this work, future research should extend environmental studies to include long-term storage conditions and measurements of the glass transition temperature. It should also evaluate the powder flow performance at pilot scale to validate lab-based correlations. Furthermore, the study would benefit greatly from multiple measurement for statistical robustness. Additionally, image analysis in combination with rheological measurements to gain a better understanding of particle shape on flowability. Lastly, studies into the effect of fat content on flowability would help enhance the results and hopefully provide further insights into the differences in physical characteristics between in-house and external suppliers' samples.

References

1. Suhag, R., Kellil, A. & Razem, M. Factors Influencing Food Powder Flowability. *Powders 2024, Vol. 3, Pages 65-76* **3,** 65–76. ISSN: 2674-0516. doi:10.3390/POWDERS3010006. https://www.mdpi.com/2674-0516/3/1/6/htm%20https://www.mdpi.com/2674-0516/3/1/6 (Feb. 2024).
2. *FT4 Powder Rheometer | External Variables* https://www.freemantech.co.uk/powder-testing/ft4-powder-rheometer-powder-flow-tester/external-variables.
3. Larsson, A. *Evaluation of Natural Anti--caking Agents in Spices and Spice Blends For a Consumer--friendly Labeling of Spice Products* tech. rep. ().
4. Yu, H. & MacGregor, J. F. Multivariate image analysis and regression for prediction of coating content and distribution in the production of snack foods. *Chemometrics and Intelligent Laboratory Systems* **67,** 125–144. ISSN: 01697439. doi:10.1016/S0169-7439(03)00065-0 (Aug. 2003).
5. Leturia, M., Benali, M., Lagarde, S., Ronga, I. & Saleh, K. Characterization of flow properties of cohesive powders: A comparative study of traditional and new testing methods. *Powder Technology* **253,** 406–423. ISSN: 0032-5910. doi:10.1016/J.POWTEC.2013.11.045 (Feb. 2014).
6. Zheng, Q. J. *et al.* Interparticle forces and their effects in particulate systems. *Powder Technology* **436.** ISSN: 1873328X. doi:10.1016/j.powtec.2024.119445 (Mar. 2024).
7. *Powder Rheology | Powder Flowability | Powder Behaviour* https://www.freemantech.co.uk/learn/powder-rheology.
8. Aguilera, J. M., del Valle, J. M. & Karel, M. Caking phenomena in amorphous food powders. *Trends in Food Science & Technology* **6,** 149–155. ISSN: 0924-2244. doi:10.1016/S0924-2244(00)89023-8 (May 1995).
9. Caking in Food Powders.
10. Chen, M. *et al.* Caking of crystals: Characterization, mechanisms and prevention. *Powder Technology* **337,** 51–67. ISSN: 0032-5910. doi:10.1016/J.POWTEC.2017.04.052 (Sept. 2018).
11. Carpin, M. *et al. Caking of lactose: A critical review* July 2016. doi:10.1016/j.tifs.2016.04.002.
12. Alvino Granados, A. E., Mochizuki, T. & Kawai, K. Effect of Glass Transition Temperature Range on the Caking Behavior of Freeze-dried Carbohydrate Blend Powders. *Food Engineering Reviews* **13,** 204–214. ISSN: 18667929. doi:10.1007/S12393-020-09226-Z/METRICS. https://link.springer.com/article/10.1007/s12393-020-09226-z (Mar. 2021).
13. Lipasek, R. A., Ortiz, J. C., Taylor, L. S. & Mauer, L. J. Effects of anticaking agents and storage conditions on the moisture sorption, caking, and flowability of deliquescent ingredients. *Food Research International* **45,** 369–380. ISSN: 09639969. doi:10.1016/j.foodres.2011.10.037 (Jan. 2012).
14. Younes, M. *et al.* Re-evaluation of calcium silicate (E 552), magnesium silicate (E 553a(i)), magnesium trisilicate (E 553a(ii)) and talc (E 553b) as food additives. *EFSA Journal* **16,** e05375. ISSN: 1831-4732. doi:10.2903/J.EFSA.2018.5375. /doi/pdf/10.2903/j.efsa.2018.5375%20https://onlinelibrary.wiley.com/doi/abs/10.2903/j.efsa.2018.5375%20https://efsa.onlinelibrary.wiley.com/doi/10.2903/j.efsa.2018.5375 (Aug. 2018).
15. Younes, M. *et al.* Re-evaluation of silicon dioxide (E 551) as a food additive. *EFSA Journal* **16.** ISSN: 18314732. doi:10.2903/j.efsa.2018.5088 (Jan. 2018).
16. Ratanatriwong, P. & Barringer, S. Particle size, cohesiveness and charging effects on electrostatic and nonelectrostatic powder coating. *Journal of Electrostatics* **65,** 704–708. ISSN: 0304-3886. doi:10.1016/J.ELSTAT.2007.05.005. https://www.sciencedirect.com/science/article/pii/S0304388607000666 (Oct. 2007).
17. Xu, G. *et al.* Investigation on characterization of powder flowability using different testing methods. *Experimental Thermal and Fluid Science* **92,** 390–401. ISSN: 0894-1777. doi:10.1016/J.EXPTHERMFLUSCI.2017.11.008 (Apr. 2018).
18. Brika, S. E., Letenneur, M., Dion, C. A. & Brailovski, V. Influence of particle morphology and size distribution on the powder flowability and laser powder bed fusion manufacturability of Ti-6Al-4V alloy. *Additive Manufacturing* **31,** 100929. ISSN: 22148604. doi:10.1016/j.addma.2019.100929 (Jan. 2020).

19. O'Donoghue, L. T. *et al.* Influence of particle size on the physicochemical properties and stickiness of dairy powders. *International Dairy Journal* **98,** 54–63. ISSN: 09586946. doi:10.1016/j.idairyj.2019.07.002 (Nov. 2019).

20. Hogan, S. A. & O'Callaghan, D. J. Influence of milk proteins on the development of lactose-induced stickiness in dairy powders. *International Dairy Journal* **20,** 212–221. ISSN: 09586946. doi:10.1016/j.idairyj.2009.11.002 (Mar. 2010).

21. Bhattacharjee, T. *et al.* Effects of particle size, distribution, and morphology on bulk shear behavior of milled loblolly pine. *Powder Technology* **457.** ISSN: 1873328X. doi:10.1016/j.powtec.2025.120911 (May 2025).

22. Lin, L., Yu, M., Liu, Y., Chen, X. & Luo, Z. H. A comparative analysis of techniques for characterizing particle-scale adhesion and cohesion. *Powder Technology* **447.** ISSN: 1873328X. doi:10.1016/j.powtec.2024.120203 (Nov. 2024).

23. Zegzulka, J., Gelnar, D., Jezerska, L., Prokes, R. & Rozbroj, J. Characterization and flowability methods for metal powders. *Scientific Reports* **10,** 1–19. ISSN: 20452322. doi:10.1038/S41598-020-77974-3;SUBJMETA=166,301,419,639,705,766;KWRD=ENGINEERING,MATERIALS+SCIENCE,MATHEMATICS+AND+COMPUTING,PARTICLE+PHYSICS. https://www.nature.com/articles/s41598-020-77974-3 (Dec. 2020).

24. Joo, Y. J., Soreghan, A. M., Madden, M. E. & Soreghan, G. S. Quantification of particle shape by an automated image analysis system: a case study in natural sediment samples from extreme climates. *Geosciences Journal* **22,** 525–532. ISSN: 15987477. doi:10.1007/s12303-018-0025-0 (Aug. 2018).

25. *Angle of Repose Explained* https://www.lfacapsulefillers.com/videos/angle-of-repose-explained.

26. Brown, C. J. & Nielsen, J. *Silos : Fundamentals of Theory, Behaviour and Design* ISBN: 9781482271744. http://ebookcentral.proquest.com/lib/chalmers/detail.action?docID=5379186 (Taylor & Francis Group, Milton, UNITED KINGDOM, 1998).

27. Freeman Technology. *Powder Flow Testing with the FT4 Powder Rheometer* https://www.freemantech.co.uk/powder-testing/ft4-powder-rheometer-powder-flow-tester.

28. *FT4 Powder Rheometer | Shear Testing | Shear Cell* https://www.freemantech.co.uk/powder-testing/ft4-powder-rheometer-powder-flow-tester/shear-testing.

29. *Yield point | Stress-Strain, Plasticity & Deformation | Britannica* https://www.britannica.com/science/yield-point.

30. *Understanding Mohr's Circle and Stress Transformation | The Efficient Engineer* https://efficientengineer.com/mohrs-circle/.

31. *FT4 Powder Rheometer | Bulk Properties* https://www.freemantech.co.uk/powder-testing/ft4-powder-rheometer-powder-flow-tester/bulk-properties.

32. Freeman Technology. *Dynamic Methodology* 2025. https://www.freemantech.co.uk/powder-testing/ft4-powder-rheometer-powder-flow-tester/dynamic-methodology.

33. Marchetti, L., Mellin, P. & Neil Hulme, C. Negative impact of humidity on the flowability of steel powders. *Particulate Science and Technology* **40,** 722–736. ISSN: 15480046. doi:10.1080/02726351.2021.1995091 (2022).

34. Hausmann, A. *et al.* The importance of humidity control in powder rheometer studies. *Powder Technology* **421,** 118425. ISSN: 0032-5910. doi:10.1016/J.POWTEC.2023.118425 (May 2023).

35. Rowley, G. & Mackin, L. A. The effect of moisture sorption on electrostatic charging of selected pharmaceutical excipient powders. *Powder Technology* **135-136,** 50–58. ISSN: 00325910. doi:10.1016/j.powtec.2003.08.003 (Oct. 2003).

36. Anantawittayanon, S., Mochizuki, T. & Kawai, K. Effects of Water Activity and Temperature on the Caking Properties of Amorphous Carbohydrate Powders. *Journal of Applied Glycoscience* **72,** 7201103. ISSN: 1344-7882. doi:10.5458/JAG.7201103. https://www.jstage.jst.go.jp/article/jag/72/1/72_7201103/_article (Feb. 2025).

37. Mathlouthi, M. Water content, water activity, water structure and the stability of foodstuffs. *Food Control* **12,** 409–417. ISSN: 0956-7135. doi:10.1016/S0956-7135(01)00032-9. https://www.sciencedirect.com/science/article/pii/S0956713501000329?casa_token=joB-GAWveNOAAAAA:WOrCXQltqJm4u4NOFzjC3u01d8qqyaLXL (Oct. 2001).

38. Dubey, A. Powder flow and blending. *Predictive Modeling of Pharmaceutical Unit Operations,* 39–69. doi:10.1016/B978-0-08-100154-7.00003-X. https://www.sciencedirect.com/science/article/pii/B978008100154700003X (Jan. 2017).

39. *Understanding the difference between high shear and low shear in industrial mixing applications | Processing Magazine* https://www.processingmagazine.com/mixing-blending-size-reduction/article/55245187/understanding-the-difference-between-high-shear-and-low-shear-in-industrial-mixing-applications.

40. *Statistics Calculator [t-Test, Chi-square, Regression, Correlation,...]* https://datatab.net/.

41. Fitzpatrick, J., Barry, K., Delaney, C. & Keogh, K. *Assessment of the flowability of spray-dried milk powders for chocolate manufacture* in *Lait* **85** (July 2005), 269–277. doi:10.1051/lait:2005012.

42. Eggers, T., Rackl, H. & von Lacroix, F. Investigation of the Influence of the Mixing Process on the Powder Characteristics for Cyclic Reuse in Selective Laser Sintering. *Powders* **2,** 32–46. doi:10.3390/powders2010003 (Jan. 2023).

43. Hertel, M. *et al.* The influence of high shear mixing on ternary dry powder inhaler formulations. *International Journal of Pharmaceutics* **534,** 242–250. ISSN: 0378-5173. doi:10.1016/J.IJPHARM.2017.10.033. https://www.sciencedirect.com/science/article/pii/S0378517317310128 (Dec. 2017).

A FT4 powder rheometer® user manual

The following sections detail how to operate the FT4 powder rheometer®.

A.1 Materials

- Powder scooper or regular spoon
- Duster
- Computer with MS excel, "Powder Rheometer," and "Data Analysis v4" software installed and connected to the FT4 Powder Rheometer®
- FT4™
- FT4™ Accessory Kit (48 mm blade, vented piston head)
- FT4™ Shear cell head Accessory Kit
- Aeration control unit
- Air compressor for aeration test
- FFP mask by Arnitech
- Gas spray
- Ethanol

A.2 Starting and shutting down FT4 Powder Rheometer®

1. Press the power button located on the upper right side of the machine which will consequently turn on the PC.
2. On the computer screen, click the FT4 powder rheometer® program.
3. Login with username and password.
4. To shut down, remove any attachments on the powder rheometer. Shut down using the PC.

A.3 Aeration

Aeration is a dynamic flow measurement that determines how easily air can be introduced to a powder by measuring the reduction of flow energy when air is supplied to it. Cohesive powders are generally less aerable as it requires more air to break apart the cohesive forces between the particles. It uses a 48 mm blade as a starting accessory and a 50 mm x 260 ml vessel with a metal base. It also utilizes an aeration control unit connected to a gas supply pump. It is run by a user defined program "**50mm_Aeration_6(C+T)_20**" where 6 denotes the number of cycles, C is the conditioning cycle, T is the test cycle and 20 is the maximum air velocity of 20 mm/s. The test cycles are carried out at a blade tipspeed of 100 mm/s.

1. Click "stand method", click user methodologies tab and pick the "**50mm_Aeration_6(C+T)_20**" program.
2. Assemble a 260 ml x 50 mm vessel with the clamp (?) and attach the funnel on top. Screw the 48 mm blade onto the machine
3. Check the box on all the necessary parts.
4. In the next view window tare the vessel with the funnel then remove the vessel to fill it with sample prepared on the next step.
5. Assemble a 160 ml x 50 mm split vessel and fill slightly above 160 ml of the sample. Split the vessel to get the exact amount 160 ml sample.
6. Pour the sample into the 260 ml x 50 mm vessel and then place it back on the machine. Screw it in place.
7. Pull down safety cover and press "record sample mass".

8. On the window, add information about batch number, date, and batch name.
9. Click done and let the machine run the test to completion.
10. Once done, save the results in the appropiate folder with the correct replicate number.

A.4 Shear cell test

The shear cell is a test to measure the flowability of a powder that previously has been at rest[2]. Powders that have been stored consolidate, thus becoming more compact.The importance of this test is to determine whether storage might play a factor in the decreased flowability of the powder during processing.The shear cell test uses the standard program **50mm_Shear_6kPa** with a 48 mm blade as a starting accessory, a 50 mm x 85 ml split vessel with a blue base that is included in the shear cell accessory kit. The 6 kPa refers to the pre-consolidation stress level.

1. Click ”Standard Program”, click ”shear cell” in the dynamic flow methodologies.
2. Choose 6 kPa in the 50 mm vessel column.
3. Assemble a 85 ml x 50 mm vessel split vessel with the clamp (?) and attach the funnel on top. Screw the 48 mm blade into the spindle on the machine.
4. Check the box on all the necessary parts in the **Vessel & Blade Confirmation**.
5. In the next view window, **Vessel Tare**, tare the empty vessel including the funnel then remove the vessel from the machine to fill it with the sample.
6. Fill a little over the 85 ml mark of the sample into the vessel.
7. Place the vessel on the machine and screw it in place.
8. Pull down safety cover and press ”record sample mass”.
9. On the window **Standard Test Confirmation**, add information about batch code, test date, and material.
10. Click ”Start test” and the rheometer will run a pre-conditioning process.
11. Once completed, an on-screen prompt will appear. Lift up the safety cover and change 48 mm blade to vented piston.
12. Pull down the safety door, click ”OK”. The rheometer will compact the powder.
13. A second on-prompt box will appear once the compacting process is complete. Lift the safety cover.
14. Remove the funnel, split the vessel and change to the shear cell head. Split the vessel by pressing down on the white spring and moving the upper part of the vessel to the side. Use a petri dish or equivalent to catch the excess powder and return the excess powder back into the sample bag.
15. Pull down safety cover, click ”OK” and rheometer will start the shear cell test.

A.5 Compressibility

Compressibility is a test to determine how density changes as a function of applied normal stress. The test helps to create a correlation between the interaction of cohesive powers in the powder and how they may cause the powder to consolidate. Powers with high compressibility will be cohesive in nature. Compressibility is a measure of the bulk density in the sample. In the FT4, the standard program **50mm_Compressibility_0p5_15kPa** was used with a 48 mm blade as a starting accessory and a 50 mm x 85 ml split vessel with a white base. The following instructions detail the steps carried out by the operator.

1. Click ”standard method”, click ”compressibility” in the bulk measurements and choose 50 mm vessel.
2. Assemble 50 mm x 85 ml split vessel and screw 48 mm blade into the spindle on the machine.
3. Check the box with all the necessary parts in the **Vessel Blade Confirmation**.
4. In the next view window, **Vessel Tare**, tare the empty vessel including the funnel.

5. Remove the vessel from the machine and fill it with the sample, a little bit in excess over the split mark.
6. Place the vessel on the machine and screw it in place.
7. Pull down safety cover and click "Record sample mass" on the screen.
8. On the window **Standard Test Confirmation**, add all necessary information.
9. Press "Start" and the rheometer will proceed with the pre-conditioning step, wait until it is completed to move on to the next step.
10. Once completed, an on-screen prompt will appear. Lift the safety cover, remove funnel and split the vessel. Split the vessel by pressing down on the white spring and moving the upper part of the vessel to the side. Use a petri dish or equivalent to catch the excess powder and return the excess powder back into the sample bag.
11. Return the upper part of the vessel back into its former position, pushing down the white spring to secure it back in place.
12. Change to a vented piston by unscrewing the 48 mm blade from the spindle and replacing it with the vented piston..
13. Pull down safety cover and press "OK" on the screen to proceed to the next step. The rheometer will begin the compressibility test.
14. Once finished, save results and remove the piston and vessel from the rheometer. Discard the sample and clean the vessel and accessories to prepare for the next test. Dust off any excess powder and use an oil free gas spray to remove any remaining powder in the vessel.

A.6 Basic flow energy (BFE)

The basic flowability energy (BFE) uses a 48 mm blade as a starting accessory and a 50 mm x 160 ml split vessel with a white base. The program used is user defined **50mm_1C_split_1T_2C + levelling** which references to 1 conditioning cycle, splitting of the sample to provide the exact volume of the sample, 1 test cycle at 100 mm/s tipspeed and 2 conditioning cycles and a final levelling.

1. Select **Advanced Program Selection**, click to User Test Programs" and select **50mm_1C_split_1T_2C + levelling**. Click "Run".
2. Assemble 50 mm x 160 ml split vessel and screw 48 mm blade into the spindle of the rheometer.
3. Check the box with all the necessary accessories in the **Vessel Blade Confirmation**.
4. In the next view window, **Vessel Tare**, tare the empty vessel including the funnel.
5. Remove the vessel from the machine and fill it with the sample, a little bit in excess over the split mark.
6. Return the vessel back to the machine and screw it in place. Pull down the safety cover and press "Record sample mass"
7. In the next window, add sample name, batch number and test date in the relevant text fields. Press "Start test" and the rheometer will proceed to the preconditioning step.
8. Once the preconditioning step is completed, lift the safety cover.
9. Split the vessel by pressing down on the white spring and sliding the upper part of the vessel to the side. Collect the excess sample in a petri dish and return the sample into the bag.
10. Slide the upper part vessel back into place. Pull down safety cover and place "OK" to begin the test.
11. The rheometer will run the test to completion.
12. Once completed, lift the safety cover and save the results. Unscrew the blade and vessel and discard the tested sample. Dust off any powder on the rheometer, vessel and blade. Use an gas spray to remove any remaining powder.

B Raw experimental data

B.1 Particle size distribution

Mesh size (μm)	**Low shear**	**High shear**
<0.15	17.52	3.33
<0.15	4.87	2.73
0.15	86.7	84.7
0.15	76.7	88.46
0.3	4.91	6.88
0.3	7.02	11.12
0.4	1.08	1.21
0.4	0.62	1.16
0.5	0.24	0.17
0.5	0.33	0.25

Table 27: Raw data from the particle sieve analysis of samples subjected to low- and high shear mixing.

B.2 Particle morphology

	Diameter					**Circularity**		**Convexity**		**Elongation**	
	ND mean	VD mean	dn(0.1)	dn(0.5)	dn(0.9)	ND mean	VD mean	ND mean	VD mean	ND mean	VD mean
SP-7	16.06	152.3	2.12	11.24	33.39	0.86	0.895	0.982	0.984	0.208	0.468
SP-7	15.02	116.2	1.99	8.57	34.34	0.821	0.879	0.972	0.976	0.245	0.53
SP-6	23.15	154	5.19	17.97	43.04	0.854	0.89	0.982	0.984	0.231	0.456
SP-6	16.42	204.1	1.98	11.48	33.63	0.841	0.888	0.979	0.982	0.233	0.478
SM-1.3%	28.38	196.6	5.61	21.39	54.5	0.829	0.877	0.973	0.977	0.235	0.479
SM-1.3%	25.66	176.8	3.64	19.93	50.5	0.833	0.878	0.972	0.976	0.227	0.473
SP-8	16.7	148.5	4.13	11.84	32.95	0.889	0.918	0.986	0.988	0.179	0.429
SP-8	8.19	158.2	3.47	6.74	12.51	0.906	0.922	0.988	0.989	0.162	0.373
SM-1.75%	11.45	183.9	2.14	8.25	21.54	0.864	0.895	0.981	0.983	0.204	0.447
SM-1.75%	10.88	163.3	2.56	7.83	19.68	0.842	0.89	0.97	0.975	0.192	0.444

Table 28: Morphological characteristics of samples with duplicate measurements. Mean values for particle size, circularity, elongation, and convexity are given based on both number distribution (ND) and volume distribution(VD). Additionally for the particle size, the percentiles d(0.1), d(0.5) and d(0.9) based on ND is given.

B.3 Statistical analysis

	Sum of Squares	**df**	**Mean Square**	**F**	**p**
Sample	0.01	3	0	54.88	<.001
Residual	0	8	0		
Total	0.01	11			

Table 29: One way ANOVA for samples subjected to wimter conditions tested day 1

	Sum of Squares	**df**	**Mean Square**	**F**	**p**
Sample	0	3	0	7.15	.012
Residual	0	8	0		
Total	0	11			

Table 30: One way ANOVA for samples subjected to summer conditions tested day 1

	Sum of Squares	df	Mean Square	F	p
Sample	0.01	3	0	3592.7	<.001
Residual	0	8	0		
Total	0.01	11			

Table 31: One way ANOVA for samples subjected to summer conditions tested day 14

	Sum of Squares	df	Mean Square	F	p
Condition	0.03	2	0.01	12.01	<.001
Residual	0.03	21	0		
Total	0.05	23			

Table 32: One way ANOVA for samples subjected to both conditions (summer and winter) tested at day 1

	Sum of Squares	df	Mean Square	F	p
Condition	0.02	2	0.01	4.33	.027
Residual	0.04	21	0		
Total	0.06	23			

Table 33: One way ANOVA for samples subjected to both conditions (summer and winter) tested at day 14

B.4 Water activity

Winter day 1 (%-SiO2)	**Water activity (Aw) mean**
0% REF	0.212 (±0.012)
1.30%	0.237 ((±0.001)
1.50%	0.180 (±0.003)
1.75%	0.182 (±0.001)

Summer day 1 (%-SiO2)	**Water activity (Aw) mean**
0% REF	0.307 (±0.004)
1.30%	0.310 (±0.003)
1.50%	0.311 (±0.0)
1.75%	0.296 (±0.007)

Winter day 14 (%-SiO2)	**Water activity (Aw) mean**
0% REF	0.313 (±0.0)
1.30%	0.225 (±0.016)
1.50%	0.203 (±0.004)
1.75%	0.205 (±0.002)

Summer day 14 (%-SiO2)	**Water activity (Aw) mean**
0% REF	0.227 (±0.001)
1.30%	0.306 (±0.002)
1.50%	0.300 (±0.0)
1.75%	0.315 (±0.001)

Table 34: Water activity, average of triplicate measurements

DEPARTMENT OF FOOD AND NUTRITION SCIENCE
CHALMERS UNIVERSITY OF TECHNOLOGY
Gothenburg, Sweden 2025
www.chalmers.se

CHALMERS
UNIVERSITY OF TECHNOLOGY